

Journal of Visualized Experiments

A Multilayer Microfluidic Platform for the Conduction of Prolonged Cell-Free Gene Expression

--Manuscript Draft--

Article Type:	Invited Methods Article - JoVE Produced Video
Manuscript Number:	JoVE59655
Full Title:	A Multilayer Microfluidic Platform for the Conduction of Prolonged Cell-Free Gene Expression
Order of Authors:	Ardjan J. van der Linden Maaruthy Yelleswarapu Pascal A. Pieters Zoe Swank Wilhelm T. S. Huck Sebastian J. Maerkl Tom F. A. de Greef
Keywords:	Microfluidics, in vitro transcription and translation, synthetic biology, prolonged reactions, micro-reactors, protein expression
Abstract:	The limitations of cell-based synthetic biology are becoming increasingly apparent as researchers strive to develop larger and more complex synthetic genetic regulatory circuits. The analysis of synthetic genetic regulatory networks <i>in vivo</i> is time consuming and suffers from a lack of environmental control, with exogenous synthetic components interacting with host processes resulting in undesired behaviour. To overcome these issues, the cell-free characterization of novel circuitry is becoming more prevalent. In vitro transcription and translation (IVTT) mixtures allow the regulation of the experimental environment and can be optimised for each unique system. The protocols presented here detail the fabrication of a multilayer microfluidic device which can be utilised to sustain IVTT reactions for prolonged durations. In contrast to batch reactions, where resources are depleted over time and (by-) products accumulate, the use of microfluidic devices allows the replenishment of resources as well as the removal of reaction products. In this manner, the cellular environment is emulated by maintaining an out-of-equilibrium environment within which the dynamic behaviour of the circuits can be investigated over extended periods of time. To fully exploit the multilayer microfluidic devices, hardware and software have been integrated to automate the IVTT reactions. By combining IVTT reactions with the microfluidic platform presented here, it becomes possible to comprehensively analyse complex network behaviours, furthering our understanding of the mechanisms which regulate cellular processes.

1 Title

2 A Multilayer Microfluidic Platform for the Conduction of Prolonged Cell-Free Gene Expression

4 Authors & Affiliations

5 Ardjan J van der Linden¹, Maaruthy Yelleswarapu², Pascal A Pieters¹, Zoe Swank³, Wilhelm T S

6 Huck², Sebastian J Maerkli^{3*}, Tom F A de Greef^{1,2*}

7 ¹ Institute for Complex Molecular Systems, Department of Biomedical Engineering,

8 Computational Biology Group, Eindhoven University of Technology, Eindhoven, The

9 Netherlands

10 ² Institute for Molecules and Materials, Radboud University, Nijmegen, The Netherlands

11 ³ Institute of Bioengineering, School of Engineering École Polytechnique Fédérale de Lausanne

12 (EPFL), Lausanne, Switzerland

14 Corresponding Authors:

15 Tom F A de Greef

16 Email Address: T.F.A.d.Greef@tue.nl

18 Sebastian J Maerkli

19 Email Address: sebastian.maerkli@epfl.ch

21 Email Addresses of Co-authors:

22 Ardjan van der Linden (a.j.v.d.linden@tue.nl)

23 Maaruthy Yelleswarapu (m.Yelleswarapu@science.ru.nl)

24 Pascal Pieters (p.a.pieters@tue.nl)

25 Zoe Swank (zoe.Swank@epfl.ch)

26 Wilhelm Huck (w.huck@science.ru.nl)

28 Key Words

29 Microfluidics, *in vitro* transcription and translation, synthetic biology, prolonged reactions, micro-reactors, protein expression

32 Short Abstract

33 The fabrication process of a PDMS-based, multilayer, microfluidic device with which *in vitro*
34 transcription and translation (IVTT) reactions can be performed is presented. Furthermore, a
35 comprehensive overview of the hardware and software required to automate and maintain these
36 reactions for prolonged durations is provided.

38 Long Abstract

39 The limitations of cell-based synthetic biology are becoming increasingly apparent as researchers
40 strive to develop larger and more complex synthetic genetic regulatory circuits. The analysis of
41 synthetic genetic regulatory networks *in vivo* is time consuming and suffers from a lack of
42 environmental control, with exogenous synthetic components interacting with host processes
43 resulting in undesired behaviour. To overcome these issues, the cell-free characterization of
44 novel circuitry is becoming more prevalent. *In vitro* transcription and translation (IVTT) mixtures

allow the regulation of the experimental environment and can be optimised for each unique system. The protocols presented here detail the fabrication of a multilayer microfluidic device which can be utilised to sustain IVTT reactions for prolonged durations. In contrast to batch reactions, where resources are depleted over time and (by-) products accumulate, the use of microfluidic devices allows the replenishment of resources as well as the removal of reaction products. In this manner, the cellular environment is emulated by maintaining an out-of-equilibrium environment within which the dynamic behaviour of the circuits can be investigated over extended periods of time. To fully exploit the multilayer microfluidic devices, hardware and software have been integrated to automate the IVTT reactions. By combining IVTT reactions with the microfluidic platform presented here, it becomes possible to comprehensively analyse complex network behaviours, furthering our understanding of the mechanisms which regulate cellular processes.

57

58 **Introduction Jove Manuscript**

Cells are able to sense and respond to their environment using complex dynamic regulatory networks^{1,2}. The field of synthetic biology utilises our knowledge of the naturally occurring components comprising these networks to engineer biological systems that can expand the functionality of cells^{3,4}. Conversely, it is also possible to further our understanding of the natural networks governing life by designing simplified, synthetic analogues of existing circuits or by forward-engineering biological systems which exhibit naturally occurring behaviours. The *de novo* engineering of such biological systems is performed in a bottom-up fashion where novel genetic circuits or signalling pathways are engineered in a rational manner, using well-defined parts^{5,6}. Combining the rational design of networks with the design of biologically relevant systems enables the in-depth characterisation and study of biological regulatory systems with various levels of abstraction⁷.

70

The pioneering works of Elowitz and Leibler⁸ and Gardner *et al.*⁹ were the first to demonstrate the successful introduction of synthetic genetic networks into cellular hosts. In the following decade, numerous researchers have continued to build on these initial successes despite the emergence of several limitations regarding the introduction of synthetic circuits into cells^{7,10,11,12}. Ideally, the introduction of synthetic circuits into cellular hosts should occur in a modular fashion. Unfortunately, the complexity of the cellular environment makes this particularly challenging, with the function of many parts and networks being highly context dependent^{12,13,14}. As a result, networks often experience undesired interactions with native host componentry which can affect the function of the synthetic circuit. Similarly, components of the exogenous network can inhibit host processes, compete for shared resources within the host, and influence growth kinetics^{15–17}. Consequently, in order to rationally design and predict the behaviour of synthetic networks in an *in vivo* environment, a comprehensive model of all host and circuit-specific dynamics is required¹⁸.

84

A viable alternative to the use of cellular hosts for the characterisation of synthetic networks is the application of *in vitro* transcription and translation (IVTT) technologies. Acting as a testbed for synthetic networks, reactions are performed in solutions comprising all the components required to enable gene expression^{19–21}. In this manner, a biologically relevant, albeit artificial,

89 environment is created within which synthetic networks can be tested. A major advantage of
90 using IVTT solutions is the ability to perform reactions under user-specified conditions, with
91 researchers able to tune the precise composition of each reaction². Furthermore, the cell-free
92 approach enables high-throughput testing of synthetic networks, since it removes the need to
93 perform time-consuming cellular cloning steps. As a result, the duration of successive design –
94 build – test cycles is significantly reduced^{22–25}. The design cycle can be further accelerated by
95 utilizing cell-free cloning techniques such as the Gibson assembly to rapidly engineer novel
96 networks, and by constructing networks from linear DNA templates which – unlike the plasmids
97 required for *in vivo* testing – can be amplified via polymerase chain reactions (PCR)^{26,27}.

98
99 Batch reactions are the simplest method by which IVTT reactions can be performed, requiring a
100 single reaction vessel wherein all of the reaction components are combined²⁸. Such reactions are
101 sufficient for protein expression and basic circuit testing yet prove insufficient when attempting
102 to study the long-term dynamic behaviour of a network. Over the course of a batch reaction,
103 reagents are either depleted or undergo degradation resulting in a continuous decrease of the
104 transcription and translation rates. Furthermore, as reactions progress by-products accumulate
105 which can interfere with – or completely inhibit – the correct functioning of the network.
106 Ultimately, the use of batch reactors limits the dynamic behaviour which can be observed, with
107 negative feedback being particularly challenging to implement^{5,29}.

108
109 The versatility of IVTT systems enables multiple alternative methods by which prolonged IVTT
110 reactions can be performed, ranging from continuous flow to droplet based methods as well as
111 simpler dialysis approaches^{2,23,30,31}. The application of microfluidic devices offers users increased
112 control over their reactions whilst increasing the throughput and minimizing costs^{28,32,33}. In 2013,
113 Maerkl *et al.* presented a multi-layered microfluidic device designed specifically for conducting
114 prolonged IVTT reactions^{29,34}. The use of multi-layered microfluidic devices permits direct control
115 over fluid flow, allowing for the redirection of flow as well as isolation of fluid in specific regions
116 of the device^{35,36}. These isolated regions can function as independent nanoliter-scale reaction
117 chambers wherein IVTT reactions can be performed. Over the course of a single IVTT reaction,
118 periodic injections of fresh reagents into the reactor are used to replenish IVTT components and
119 DNA templates. Simultaneously, an equal volume of the old reaction solution is displaced,
120 removing reaction products. In this manner, an out-of-equilibrium environment is maintained
121 where the basal transcription and translation rates remain in steady-state, prolonging the
122 lifetime of IVTT reactions and allowing rich dynamic behaviours to occur. By applying this
123 approach, researchers are able to investigate the kinetic rates of the individual processes
124 occurring within a specific circuit, aiding in the forward-engineering of novel genetic networks.
125 For instance, Niederholtmeyer *et al.* implemented this approach to characterise various elements
126 of a genetic ring oscillator, determining the kinetic rates thereof²⁹. In further studies,
127 Yelleswarapu *et al.* showed that the kinetic rates of a σ28 factor determined under batch
128 conditions were insufficient to describe the behaviour of a σ28-based oscillator, and that the
129 addition of flow-based data improved model predictions of the network behaviour³⁷.

130
131 The goal of this manuscript is to present a complete protocol for the fabrication of multilayer
132 microfluidic devices capable of performing long-term IVTT reactions. In addition, this manuscript

133 will describe all of the hardware and software required to perform prolonged IVTT reactions. The
134 actuation of the microfluidic device - necessary to control the flow of fluids therein - is achieved
135 using a series of pneumatic valves which connect directly to the microfluidic devices via lengths
136 of tubing. In turn, the pneumatic valves are controlled from a virtual control panel, which was
137 designed using the LabVIEW environment. Fluid flow within the microfluidic devices is achieved
138 using continuous pressure which is provided by a commercially available pressure regulation
139 system. IVTT reactions are typically performed between 29 °C and 37 °C and a microscope
140 incubator is used to regulate the temperature during reactions. However, the functionality of the
141 IVTT mixture gradually degrades when stored above 4 °C. As such, this manuscript will expand
142 upon the off-chip cooling system used to cool the IVTT mixture prior to injection into the
143 microfluidic device. In conclusion, this manuscript provides a comprehensive overview of the
144 procedures required to successfully perform prolonged IVTT reactions using a microfluidic flow
145 reactor such that other researchers will be able to replicate this technology with relative ease.
146

147 **Protocols**

148 **1. Wafer Preparation - Flow Layer**

149 Our protocols are specific for to AZ 40XT positive photoresist. Other positive photoresists can
150 be used, however the specific spin speeds, baking temperatures, and baking times will vary.

151 The microfluidic device design provided by Niederholtmeyer *et al.*²⁹ is linked in the Materials.

152 1.1 Place a clean silicon wafer in a preheated oven set to 250 °C and leave the wafer to dehydrate
153 overnight (~16 h).

154 Note: It is also possible to prime the wafer using HMDS vapour deposition, however this is
155 not necessary if the wafer is sufficiently dehydrated.

156 1.2 Remove the silicon wafer from the oven, allowing it to cool to room temperature before
157 placing proceeding with the spin coating. Apply 3-4 mL of AZ 40XT photoresist to the centre
158 of the wafer. To obtain a feature height of 25 µm apply the following spin protocol:

159 1.2.1 Spin for 20 s at 500 rpm using an acceleration of 110 rpm/s.

160 1.2.2 Spin for 30 s at 3100 rpm using an acceleration of 300 rpm/s.

161 1.2.3 Decelerate the wafer using a deceleration of 200 rpm/s.

162 1.3 Using a microfiber tissue carefully remove any edge beading which may have occurred
163 during the spin coating.

164 1.4 Soft bake using two separate hot plates set to 70 °C and 120 °C in the following manner:

165 1.4.1 Allow the wafer to sit at 70 °C for a duration of 30 s.

166 1.4.2 Transfer the wafer to the 120 °C hot plate and allow it to rest here for 3.5 min.

167 1.4.3 Return the wafer to the 70 °C hot plate and let it rest here for 30 s.

168 1.5 Remove the wafer from the hot plate and allow it to cool to room temperature. Ensure that
169 the wafer is not subjected to sudden temperature shocks (i.e. do not place the wafer directly
170 on a cool surface, instead buffer the wafer using a stack of microfiber tissues).

171 1.6 Place the photomask (emulsion side down) onto the photoresist film and place the wafer
172 underneath the UV light source. Expose the wafer using a UV lamp until a total exposure of
173 200 mJ/cm² is achieved.

174 1.7 Post-exposure bake using two hot plates (70 °C and 105 °C) in the following manner:

175 1.7.1 Allow the wafer to sit at 70 °C for 20 s

176 1.7.2 Transfer the wafer to 105 °C and leave here for 40 s.

- 177 1.7.3 Return the wafer to 70 °C for a further 20 s to complete the post exposure bake.
- 178 1.8 Allow the wafer to cool to room temperature on a stack of microfiber tissues. Develop the
179 wafer by transferring it to a petri dish filled with AZ 716 MIF developer to start the
180 development process. Development is accelerated when performed on a benchtop shaker
181 and the entire wafer is submerged in the developer.
- 182 1.9 Rinse the wafer with distilled water and use a stereo microscope to check the wafer surface
183 for any photoresist residue. If photoresist residue can be seen, then return the wafer to the
184 developer.
- 185 1.10 Reflow the positive photoresist by placing the wafer atop a hot plate set at 110 °C for 25
186 min. This process will result in rounded features as well as annealing any cracks that may
187 have appeared during the fabrication process.
- 188 1.11 Silanize the wafer to prevent the adhesion of PDMS during the soft-lithography processes.
189 Pipet 2-3 droplets (per wafer) of the silane into a small glass vial. Place this vial, along with
190 the wafer into a desiccator and pull vacuum for 5-10 min. Seal the desiccator and leave the
191 wafer under vacuum for a period of 12 – 16 h.
192 CAUTION: The silane is toxic and should not be inhaled. Take care to work in a fume hood
193 and to wear nitrile gloves when handling the silane. This includes placing the vacuum pump
194 in the fume hood when pulling vacuum on the desiccator.
- 195 1.12 Release the vacuum from the desiccator and remove the silanized wafer. Rinse the wafer
196 with water and use a steam of N₂ to dry the wafer. At this point the wafer can be placed in
197 storage until further use.

198

199 **2 Wafer Preparation - Control Layer**

200 Our protocols are specific for to SU8-3050 negative photoresist. Other negative photoresists
201 can be used, however the specific spin speeds, baking temperatures, and baking times will
202 vary. The microfluidic device design provided by Niederholtmeyer *et al.*²⁹ is linked in the
203 Materials.

- 204 2.1 Place a clean silicon wafer in a preheated oven set to 250 °C and leave the wafer to dehydrate
205 overnight (~16 h).
206 Note: It is also possible to prime the wafer using HMDS vapour deposition, however this is
207 not necessary if the wafer is sufficiently dehydrated.
- 208 2.2 Remove the silicon wafer from the oven, allowing it to cool to room temperature before
209 placing proceeding with the spin coating. Apply 5 mL of SU8 3050 photoresist to the centre
210 of the wafer. To obtain a feature height of 30 µm apply the following spin protocol:
- 211 2.2.1 Spin for 20 s at 500 rpm using an acceleration of 100 rpm/s.
- 212 2.2.2 Spin for 42 s at 4000 rpm using an acceleration of 330 rpm/s.
- 213 2.2.3 Decelerate the wafer using a deceleration of 200 rpm/s.
- 214 2.3 Using a microfiber tissue carefully remove any edge beading which may have occurred during
215 the spin coating.
- 216 2.4 Soft bake using two separate hot plates (65 °C and 95 °C) in the following manner:
- 217 2.4.1 Allow the wafer to sit at 65 °C for a duration of 30 s.
- 218 2.4.2 Carefully transfer the wafer to the 95 °C hot plate and allow it to rest here for 14 min.
- 219 2.4.3 Return the wafer to the 65 °C hot plate and let it rest here for 30 s.
- 220 2.5 Remove the wafer from the hot plate and allow it to cool to room temperature.

221 2.6 Measure the current intensity of the UV lamp before exposure and use this to determine the
222 exposure duration required to achieve a total exposure dosage of 260 mJ/cm². Place the
223 photomask (emulsion side down) onto the photoresist film and place the wafer underneath
224 the UV light source. Expose the wafer using a UV lamp until a total exposure of 260 mJ/cm²
225 is achieved.

226 2.7 Post exposure bake using two hot plates (65 °C and 95 °C) in the following manner:

227 2.7.1 Allow the wafer to sit at 65 °C for 1 min.

228 2.7.2 Transfer the wafer to 95 °C and leave here for 4.5 min.

229 2.7.3 Return the wafer to 65 °C for a further 30 s to complete the post exposure bake.

230 2.8 Allow the wafer to cool to room temperature on a stack of microfiber tissues. Develop the
231 wafer by transferring it to a petri dish filled with mrDev-600 developer to start the
232 development process. Development is accelerated when performed on a benchtop shaker
233 and the entire wafer is submerged in the developer.

234 2.9 Rinse the wafer with isopropanol and use a stereo microscope to check the wafer surface for
235 any photoresist residue. If photoresist residue can be seen, then return the wafer to the
236 developer.

237 2.10 Hard bake the photoresist by placing the wafer on a hot plate set at 150 °C for 1 h.

238 2.11 Silanize the wafer to prevent the adhesion of PDMS during the soft-lithography processes.
239 To perform the silanization, pipet 2-3 droplets (per wafer) of the silane into a small glass vial.
240 Place this vial, along with the wafer into a desiccator and pull vacuum for 5-10 min. Seal the
241 desiccator and leave the wafer under vacuum for a period of 12 – 16 h.
242 CAUTION: The silane is toxic and should not be inhaled. Take care to work in a fume hood and
243 to wear nitrile gloves when handling the silane. This includes placing the vacuum pump in the
244 fume hood when pulling vacuum on the desiccator.

245 2.12 Release the vacuum from the desiccator and remove the silanized wafer. Rinse the wafer
246 with water and use a steam of N₂ to dry the wafer. At this point the wafer can be placed in
247 storage until further use.

248 249 **3 Microfluidic Device Fabrication**

250 The soft-lithography process used to fabricate PDMS based multilayer microfluidic devices can
251 be separated into three distinct steps: 1) The PDMS preparation of both the flow and control
252 layers, 2) The alignment and bonding of the two PDMS layers, 3) The completion of the device.

253 254 **3.1 PDMS Preparation**

255 3.1.1 Prepare two separate PDMS precursor solutions, one for the flow layer and one for the
256 control layer. For each mixture combine the base agent and curing agent of the Sylgard
257 184 silicon elastomer kit in a plastic beaker and use a mixing rod to stir the two
258 components until fully mixed. The control layer requires 20 g of base agent and 1 g of
259 curing agent (20:1 ratio). The flow layer requires 40 g of the base agent and 8 g of the
260 curing agent (5:1 ratio).

261 3.1.2 Remove air from the PDMS precursor solution place the beakers in a desiccator and pull
262 vacuum until the solutions are gas free.

263 3.1.3 Place the flow layer wafer (prepared using the positive AZ 40XT photoresist) in a petri dish
264 and carefully pour the PDMS mixture over the wafer, taking care to minimise the

265 formation of air bubbles. Return the petri dish to the desiccator and pull vacuum to
266 remove any air which may have been introduced when pouring the PDMS.

- 267 3.1.4 Spin coat the control layer wafer (prepared using the negative SU8 3050 photoresist) with
268 20:1 ratio PDMS. Pour 5-10 mL of the PDMS onto the centre of the wafer and run the
269 following spin protocol (retain the left over PDMS for later use):

270 3.1.4.1 Spin for 15 s at 500 rpm using an acceleration of 100 rpm/s.

271 3.1.4.2 Spin for 45 s at 1450 rpm using an acceleration of 300 rpm/s.

272 3.1.4.3 Decelerate the wafer using a deceleration of 200 rpm/s.

273 3.1.5 Upon removing the PDMS coated wafer from the spin coater, streaks will be visible
274 around the wafer features. To ensure a homogeneous PDMS film thickness, place the
275 PDMS coated wafer on a level surface in a closed petri dish (to avoid dust contamination).
276 Let the wafer sit for 30 min.

277 3.1.6 Remove the flow layer from the desiccator and place both the flow and control layers in
278 an oven which has been preheated to 80 °C. Allow both layers to cure for 28-30 min.
279 Remove the layers when they become malleable enough to manipulate, whilst remaining
280 slightly sticky to improve the bonding process. Immediately proceed with the alignment
281 process.

282

283 **3.2 Alignment and Bonding**

284 3.2.1 Using a scalpel cut out the PDMS flow layer of each of the four devices found on the flow
285 layer wafer. Upon removing the PDMS layer from the silicon wafer, immediately cover
286 the feature side with scotch tape to avoid dust particle contamination.

287 3.2.2 Iteratively remove the tape from each of the flow layer PDMS blocks and place them on
288 the control layer PDMS, performing a rough alignment by eye.

289 3.2.3 Place the control layer wafer under a stereo microscope and adjust the position of each
290 of the flow layer blocks to align them with the control layer underneath.

291 3.2.4 After correctly aligning each device, take care to remove any air bubbles between the two
292 PDMS layers. Pour the remaining 20:1 ratio PDMS saved earlier around the aligned flow
293 layer blocks. Place 100 g weights on each of the devices to ensure sufficient contact during
294 the bonding process.

295 3.2.5 Return the devices (including the weights) to the 80 °C oven and leave them to bond for
296 at least 1.5 h and no longer than 6 h.

297

298 **3.3 Finishing the Device**

299 3.3.1 Remove the wafer from the oven and use a scalpel to cut around each individual device.
300 Peel the devices from the control layer silicon wafer, covering the feature side of each
301 device with scotch tape to prevent dust particle contamination.

302 3.3.2 Iteratively, punch a single hole for each of the 9 flow layer inlets, 24 control layer channel
303 inlets, and the single flow layer outlet for each device. Punch the device with the feature
304 side facing up, using a camera to ensure holes are punched within the feature boundaries.

305 3.3.3 For each device, clean a single microscope slide with isopropanol and acetone and dry the
306 slides under a stream of N₂. Subsequently, place the microscope slides on a hot plate set
307 to 150 °C for 15 min.

- 308 3.3.4 For each device, place a single microscope slide and a single device in the loading tray of
309 a plasma ashing. Make sure that the feature side of the PDMS device is facing upwards and
310 that the tape has been removed. Perform the oxygen plasma ashing with an ashing power
311 of 50 W for a duration of 45 sec.
- 312 3.3.5 As soon as the oxygen plasma ashing process is complete, remove the PDMS device and
313 place the device feature side down onto the microscope slide. Upon placing the PDMS
314 device onto the microscope slide, the adhesion process should be visible. Apply additional
315 pressure to regions where air pockets are visible, pushing out the air.
- 316 3.3.6 Place the bonded devices onto a hot plate set to 110 °C for an hour. Weights can be placed
317 atop the devices to improve adhesion of the device.

318

319 **4 Hardware Setup**

320 To achieve control over the microfluidic chips, numerous pieces of hardware need to be installed
321 and connected with one another. Three distinct groups of hardware are required: 1) Pneumatic
322 control system for the control channels, 2) A pneumatic pressure regulator to control flow of the
323 reaction reagents within the device, and 3) A cooling system to cool the IVTT reaction solution
324 prior to injection into the microfluidic device. A schematic overview of the hardware setup is
325 provided in **Figure 1**. It should be noted that the protocols provided here attempt to be as general
326 as possible, however certain specific pieces of equipment used throughout our research are
327 referenced. However, all hardware can be replaced by alternatives able to perform the same
328 function. In such cases, the protocols here can be used to outline the general steps needed to set
329 up the system and the requirements of each of the components. Alternative hardware setups are
330 presented by Brower *et al.*³⁸ and White and Streets³⁹.

331

332 **4.1 Pneumatic Control System (see Figure 2)**

- 333 4.1.1 For each control channel on the microfluidic device a single solenoid valve is required (for
334 the device design presented here this equates to a total of 24 solenoid valves). However,
335 three of the control channels require a lower operating pressure than the others.
336 Therefore, two separate solenoid valve arrays are required; in our setup one array
337 comprises 22 valves and the other comprises 8 valves.
- 338 4.1.2 Regulation of the solenoid valves is achieved using LabVIEW software. Within the
339 LabVIEW software, MODBUS commands are composed which are sent via a TCP
340 connection to a WAGO fieldbus controller. The manufacturers' protocol was followed to
341 establish the connection between the controller and the computer running the LabVIEW
342 software (via an Ethernet connection) as well as to power the device.
- 343 4.1.3 The fieldbus controller is expanded with eight 4-channel digital output modules. Each
344 solenoid valve presides over a connecting pin. Connect the positive wire to one of the
345 four positive outputs on one of the digital output modules whilst connecting the negative
346 wire to one of the ground ports of the digital output modules.
347 Note: To get the system to work correctly, the solenoids should be connected
348 systematically, with the first solenoid being connected to the first output port, the second
349 solenoid to the second output port and so on. In our system, the first eight output ports
350 connect to the 8-valve array, and output ports 9-30 connect to the 22-valve array.

351 4.1.4 Connect both valve arrays to a compressed air source using 1/4" tubing. Use pressure
352 regulators to set the pressure of the 22-valve array to 3 bar, and the 8-valve array to 1
353 bar.

354

355 **4.2 Flow Pressure Regulation (see Figure 3)**

- 356 4.2.1 To flow fluids through the flow layer of the microfluidic device, a commercially available
357 4-port pressure regulator is used. The output pressure of each port is regulated via
358 software provided with the pressure controller. Connect the pressure regulator to a
359 computer using the supplied USB-connector.
- 360 4.2.2 Connect the pressure regulator to a compressed air source, ensuring that the supplied
361 pressure does not exceed the maximum pressure permitted by the regulator (in our case
362 this is 800 mbar).
- 363 4.2.3 Connect a male luer to 3/32" barb connector to each of the four female luer lock output
364 ports. Connect a length of soft tubing (OD: 3 mm, ID: 1 mm, L: 10 cm) to the barb.
- 365 4.2.4 Using a second male luer to 3/32" barb connector, the open end of the soft tubing can be
366 connected to one of four reservoirs. When performing IVTT reactions these reservoirs can
367 be used to store various reaction solutions.
- 368 4.2.5 Using the supplied software, pressure can now be applied to each of the outflow ports,
369 pressurising the solutions within the reservoirs, resulting in the flow thereof into the
370 microfluidic device. The connection of the reservoirs to the microfluidic device will be
371 discussed in the section 5.2.
- 372

373 **4.2 Off-Chip Cooling Setup (see Figure 4)**

374 4.3.1 The cooling system consists of five parts; a Peltier element, a cold-plate water block, an
375 external water cooling system, a temperature monitor, and a temperature regulator.

376 4.3.2 Use PVC tubing (OD: 10 mm, ID: 6 mm) to connect the water-cooling system to the cold-
377 plate water block using compression fittings. Fill the fluid reservoir of the water-cooling
378 system with a coolant and gently tilt the unit to displace any trapped air. As the fluid level
379 in the reservoir drops, add coolant to the reservoir ensuring it remains full.

380 4.3.3 When air is no longer being displaced by tilting the unit, turn on the pump to finish filling
381 the system with coolant. Ensure that the reservoir does not empty during this process.
382 When all the air has been removed from the system, fill the reservoir to approximately
383 90-95 % of its maximal volume with coolant and seal the reservoir.

384 4.3.4 Coil PTFE tubing (OD: 0.042", ID: 0.022") onto the cold face of the Peltier element and
385 secure this with tape. Ensure that one end of the PTFE tubing is connected to the
386 reservoirs of the flow layer pressure control system (as described in section 5.3). The
387 other end of the PTFE tubing should protrude no more than 1 cm from the Peltier surface.
388 Insert a 5 – 10 cm length of PEEK tubing (OD: 0.794 mm, ID: 0.127 mm) into the protruding
389 end of the PTFE tubing. Once filled with the desired reaction solution (in our case the IVTT
390 solution) the PEEK tubing can be directly inserted into the microfluidic device. Instructions
391 regarding the loading of the reaction reagent are provided in section 5.3.

392 4.3.5 Place the hot face of the Peltier element onto the cold-plate of the water block, applying
393 sufficient thermal compound to the two faces. Ensure that the tubing, Peltier element,
394 and cooling block are in direct contact with one another at all times.

395 4.3.6 Connect the Peltier element to the temperature controller (via a serial bus connector),
396 such that the voltage supplied to the Peltier can be regulated. Securely place a thermistor
397 on the Peltier surface, connecting the output to the temperature controller. After turning
398 on the water cooler, use the temperature reading of the thermistor to regulate the
399 surface temperature of the Peltier, adapting the voltage supplied to the Peltier until the
400 temperature is stable at 4 °C. With this setup, the temperature is controlled manually,
401 and the thermistor serves only to provide a temperature measurement.

402

403 5 Preparing an Experiment

404 Prior to starting an experiment, the microfluidic device has to be prepared and the reaction
405 reagents have to be inserted into the correct tubing for injection into the device. This section will
406 discuss: 1) The connection of control channel tubing to the device, 2) The connection of uncooled
407 inflow reagents into the device, and 3) The connection of cooled inflow reagents into the device.

408

409 5.1 Connecting the control channel tubing

410 5.1.1 For each of the control channels of the microfluidic device a length of tygon tubing (OD:
411 0.06", ID: 0.02") should be cut. At one end, insert the pin of a 23 ga, 1/2" luer stub and at
412 the other insert a stainless steel connecting pin (OD: 0.65 mm, ID: 0.35 mm, L: 8 mm).

413 5.1.2 Connect the luer stub to a male luer to 3/32" barb nylon connector. The barb of the
414 connector should then be inserted into a length of polyurethane tubing (OD: 4 mm, ID:
415 2.5 mm). This polyurethane tubing can then be inserted directly into one of the solenoid
416 valves.

417 5.1.3 Attach a 23 ga, 1/2" luer stub to a syringe and insert this into a short (3-4 cm) piece of
418 tygon tubing (OD: 0.06", ID: 0.02"). Place the open end of this tubing into a reservoir of
419 milliQ water and fill the syringe with milliQ water.

420 5.1.4 Each control channel on the microfluidic device has been numbered as shown in **Figure**
421 5. For each channel (excluding control channels 1 through 3, which are not filled with
422 water), find the corresponding tubing (connected to the solenoid) and insert the metal
423 pin into the open end of the tubing attached to the syringe. Inject water into the control
424 channel tubing until half the length has been filled.

425 5.1.5 Disconnect the tubing from the syringe and insert the stainless steel connector pin into
426 the corresponding hole of the microfluidic device. Repeat until each control channel has
427 been connected to its corresponding tubing.

428 5.1.6 Use the LabVIEW software to open all the solenoid valves. This will pressurise the fluid
429 within the control channel tubing, forcing it into the microfluidic device and closing all the
430 membrane based valves within the device. An example of open and closed membranes
431 within the device are given in **Figure 7**.

432

433 5.2 Connecting uncooled reagents to the device

434 5.2.1 For each of the uncooled reagents, a length of tygon tubing (OD: 0.06", ID: 0.02") should
435 be cut. This tubing should travel from the reservoirs to the microfluidic device inlets.

436 5.2.2 Take one end of the tygon tubing and insert this into the reservoir, ensuring that the
437 tubing reaches the base of the reservoir. The reservoir tubing outlet should be tightened

438 such that an air tight seal is achieved. Insert a stainless steel connection pin (OD: 0.65
439 mm, ID: 0.35 mm, L: 8 mm) into the open end of the tygon tubing.

440 5.2.3 Attach a 23 ga, 1/2" luer stub to the end of a small (1 mL) syringe. Add a short length of
441 tygon tubing (OD: 0.06", ID: 0.02") to the luer stub. Placing the end of the tubing into the
442 desired reagent solution, fill the syringe with the reagent.

443 5.2.4 Insert the stainless steel connector pin into the polyurethane tubing connected to the
444 syringe and fill the tubing with the reagent. In the case of small reaction volumes, it may
445 occur that the fluid does not enter the reservoir. In these cases, the tygon tubing will act
446 as the reservoir; the setup does not need to be adapted. Disconnect the syringe insert the
447 connector pin into one of the flow layer inlet holes of the microfluidic device.

448 5.2.5 When pressure is applied to the reservoirs via the pressure regulator software the
449 reagents will be forced into the microfluidic device.

451 5.3 Connecting cooled fluids to the microfluidic device

452 5.3.1 The cooled reaction solution (in our case the IVTT reaction solution) should be stored in
453 the PTFE tubing coiled on the surface of the Peltier element as described in section 4.3.
454 Ensure that the water cooler and Peltier element have been turned on prior to injection,
455 with the surface temperature of the Peltier set to 4 °C. It is imperative to mount the
456 cooling setup as close to the microfluidic device as possible, minimising the uncooled
457 volume between the Peltier and the device inlet. The small inner diameter of the PEEK
458 tubing aids in reducing this dead volume further.

459 5.3.2 Connect the open end of the PTFE tubing to tygon tubing connected to one of the fluid
460 reservoirs (as described in section 5.2) using a stainless steel connector pin (OD: 0.65 mm,
461 ID: 0.35 mm, L: 8 mm).

462 5.3.3 Connect a small syringe (1 mL) to a luer stub (23 ga, 1/2") with a short length of tygon
463 tubing (OD: 0.06", ID: 0.02") attached to the end. Fill the syringe with the to-be-cooled
464 reagent via the tygon tubing.

465 5.3.4 Insert the PEEK tubing into the tygon tubing and apply constant pressure to the syringe,
466 forcing the reagent through the PEEK tubing and into the PTFE tubing. Disconnect the
467 PEEK tubing from the syringe and insert directly into one of the flow channel inlets of the
468 microfluidic device. When pressure is applied via the pressure regulator software the
469 cooled reagent will be forced into the microfluidic device.

470 6 Experimentation

471 Before any experiments can be performed with the microfluidic device, all the hardware and
472 tubing connections detailed in protocols sections 4 and 5 should be completed, and all the
473 reagents should be present in the inlets. The experimental procedure can then be divided
474 into four distinct parts: 1) the loading of the microfluidic device, 2) preparing the microscope,
475 3) the calibration of the device, and 4) performing the experiment. If desired, the LabVIEW
476 interfaced used throughout this research will be provided as supplementary information, or
477 see the Materials list)

478 6.1 Loading the microfluidic device

- 481 6.1.1 Place the microfluidic device, with all control and flow layer tubing attached into the
482 microscope stage and close any openings on the incubator. Set the ambient temperature
483 of the incubator to 29 °C. Ensure that the cooling system has been turned on and is set to
484 4 °C prior to initiating the experiment.
- 485 6.1.2 Ensure all the control channels are pressurised. The pressure of control channels 1-3
486 should be set at 1 bar, control channels 9-29 should be pressurised at 3 bar. The pressure
487 applied to the reagents should be set to between 20 and 100 mbar for all reagents.
- 488 6.1.3 Remove air from the microfluidic device using one of the reagents. To do this, ensure that
489 the outlet of the device is closed (pressurise control channel 29). Simultaneously,
490 depressurise control channels 1-3, and 15-28. Then selectively depressurise the control
491 channels of the multiplexer to allow only the selected reagent to enter the device. Use
492 the microscope to monitor the removal of air.
493 Note: In the case that reagents are not loading into the device correctly, or that the air
494 bubbles are not being removed, the pressure can be increased up to 350 mbar.
- 495 6.1.4 Ensure that all the reagents flow correctly, without introducing air - using the '*Flush*'
496 function in the LabVIEW software. Monitoring of the fluid flow can be simplified by first
497 loading a fluorophore and monitoring its displacement with each individual reagent.

500 6.2 Preparing the microscope

- 501 6.2.1 Having prepared the microfluidic device for use, images can be recorded using the
502 microscope. Prior to performing the following steps, locate any points of interest within
503 the microfluidic device, and store the locations thereof. These points will be imaged
504 during the calibration and experimental processes.
- 505 6.2.2 During the calibration and experimental procedures included within the LabVIEW
506 software, the microscope is instructed to capture images at set intervals in the protocol.
507 At these time points, the microscope is instructed to capture an image at each of the
508 locations selected in the previous step. Within our system, the LabVIEW software
509 communicates with the Nikon imaging software via the execution of a set of executables
510 which indicate when new images should be recorded, and when the imaging process has
511 been performed.
512 Note: The above process is unique to each microscope setup, and as such this
513 functionality has been modified within the provided LabVIEW interface. Provided is a
514 dummy executable, which can be modified by the end-user for compatibility with their
515 own microscope system.

517 6.3 Calibrating the microfluidic device

- 518 6.3.1 To determine the volume of fluid displaced from each reactor during a single inflow step
519 (pump sequence provided by peristaltically actuating control channels 15-17, comprising
520 6 MODBUS commands executed sequentially) a calibration is performed.
- 521 6.3.2 Determine and set the following data fields within the LabVIEW software: '*Elution Buffer
522 Channel*' – the inflow channel wherein the eluent has been inserted, '*Fluorophore
523 Channel*' – the inflow channel wherein the fluorophore has been inserted, '*Number of
524 Dilution Cycles*' – the desired number of dilutions for the calibration (default is 10

525 dilutions), ‘Number of Inflow Steps’ – the number of inflow steps per dilution cycle
526 (default is 15 steps), ‘Number of Mixing Cycles’ – how many mixing cycles are performed
527 between each dilution (default is 4 cycles), and ‘Time between Mixing Cycles’ – the waiting
528 time in seconds between successive mixing cycles (default is 0 seconds). Initiate the
529 calibration by pressing ‘Perform Calibration Experiment’.

- 530 6.3.3 During the calibration process, all the reactors are fully filled with a fluorophore and
531 images are recorded. Subsequently, a series of dilutions are performed. For each reactor,
532 the desired number of inflow steps are executed to inject the eluent into the reactor,
533 displacing a volume of the fluorophore whereby the concentration thereof in the reactors
534 is diluted. After thoroughly mixing, new images are taken. This process repeats for the set
535 ‘Number of Dilution Cycles’.

- 536 6.3.3 Upon completion of the calibration, the LabVIEW program will prompt a Matlab script to
537 run, which will guide users through a data analysis process, wherein the reduction in
538 fluorescence per dilution cycle is correlated to the number of inflow steps performed. The
539 output of this script will provide users with a value termed the ‘Refresh Ratio’ for each
540 reactor. This value indicate the fraction of the reactor volume displaced by the set
541 ‘Number of Inflow Steps’. In turn, this value will be used during experiments to determine
542 how many inflow steps are required to displace a specific reactor volume.

544 6.4 Performing the Experiment

- 545 6.4.1 Similar to the calibration, a desired experiment can be initiated using a single button on
546 the LabVIEW user interface: ‘Perform Experiment’.

- 547 6.4.2 The specific reaction protocol will determine which fields of the LabVIEW interface should
548 be set prior to the initiating the experiment. The most important setting to input is the
549 ‘Refresh Fraction [%]’, which denotes the fraction of the reactor which is displaced during
550 each round of injecting new reagents. Typically this value is set between 15 and 40 %.
551 Each of the other fields will vary depending on the experiment to be performed, and some
552 minor LabVIEW coding will be required for each novel reaction setup. The provided
553 software should provide enough information for users to create their own protocols.

- 554 6.4.3 The provided software is used to perform simple protein expression. Reactors 1 and 8 of
555 the microfluidic device are utilised as controls, while reactors 2-7 execute identical
556 experiments. Herein, 75 % of the reactors comprise IVTT solution, with the final 25 %
557 being used for milliQ water or a 2.5 nM linear DNA solution. The reactions are diluted
558 approximately every 15 minutes, with 30 % of the reactor volume being displaced during
559 each dilution. Images are recorded at the end of each dilution cycle.

561 7 Data Analysis

- 562 Matlab scripts have been provided for the analysis of the images (see supplementary files or the
563 Materials list), making use of the ‘bfopen’ Matlab package, which is required for the reviewing of
564 ‘.nd2’ files (as provided by our microscope setup). The analysis software allows user to select a
565 region of interest at each position where images were recorded, and subsequently averages the
566 fluorescence intensity at each of the positions for each recorded image. This data is provided as
567 an output and can be further analysed to view the increases or decreases in fluorescence over
568 time. The tool can also be used to select regions of background, which can be used to remove

569 any noise present on the images. The specific analysis methods will depend on the specific
570 reactions being performed, and the desired data.

571

572 **Representative Results**

573 To demonstrate the effectiveness of the multilayer microfluidic platform for the conduction of
574 IVTT experiments, the described setup was used to express the deGFP protein. The experiment
575 was conducted in the commercially available myTXTL²³ IVTT reaction mixture – comprising all the
576 necessary transcription and translation componentry – supplemented with reaction substrates
577 and DNA templates. Experiments were conducted at a temperature of 29 °C; a temperature
578 found to be optimal for the IVTT expression of proteins.

579

580 The microfluidic device possesses nine unique inlets, of which four were utilised during this
581 experiment. The first contained the commercially obtained myTXTL IVTT reaction mixture. The
582 myTXTL reaction mixture accommodates all the components required to successfully express
583 proteins, although purified GamS protein was added – at a final concentration 1.3 µM - to limit
584 the degradation of the linear DNA species during the reaction. Crucially, the IVTT mixture was
585 injected into polytetrafluoroethylene (PTFE) tubing coiled onto a Peltier element with a surface
586 temperature of 4°C to cool the solution prior to the injection thereof into the microfluidic device;
587 preventing the degradation of the reaction solution prior to its use. Micro-bore polyether ether
588 ketone (PEEK) tubing was used to connect the PTFE tubing leaving the Peltier element surface
589 with the microfluidic device, reducing the volume of the IVTT reaction mixture not being cooled.
590 The second solution inserted into the device contained the linear DNA template coding for the
591 deGFP – dissolved in milliQ water – at a concentration of 10 nM. The third solution, milliQ water,
592 served multiple purposes during the experimental procedures. Primarily, the milliQ water was
593 used to ensure that the displaced volume per dilution was equal for all reactors, acting as a
594 replacement for DNA in the control reactions. Additionally, milliQ water was also used to dilute
595 the fluorophore during the device calibration and to flush the dead volume of the device when
596 switching between reagents. The final solution inserted into the device was a purified FITC-
597 dextran solution (25 µM) required to perform the initial device calibration. The DNA, water, and
598 fluorophore solutions were injected into Tygon tubing which could subsequently be inserted into
599 one of the inflow channels of the microfluidic device as per Section 5.2 of the protocols. As such,
600 these solutions were stored at 29 °C for the entirety of the experiments.

601

602 The actuation of the control channels of the microfluidic device is achieved via custom LabVIEW
603 software where each of the control channels can be individually actuated. The execution of
604 prolonged IVTT reactions cannot be achieved via this manual process and requires the use of
605 automated protocols incorporated within the LabVIEW software. When preparing a microfluidic
606 device for experiments, similar automated protocols can be utilised to execute a number of
607 useful processes: the flushing of the device dead volume with a new reagent, the mixing of the
608 reagents within the ring reactor, and the loading of a new reagent into the reactor whilst
609 displacing an equal volume of the current solution. In addition, two complex process are
610 available: the conduction of a device calibration, and the execution of a prolonged cell-free
611 protein expression. All of the aforementioned processes can be easily executed from the main

612 LabVIEW virtual interface, alongside the ability to configure multiple parameters to vary specific
613 process settings such as the inflow channel, inflow volume, and mixing duration.

614

615 Due to fluctuations in pressure and imperfections during microfluidic device fabrication, the
616 volume of fluid displaced during a single injection cycle can vary between devices. As such, prior
617 to performing IVTT experiments, the displaced reactor volume per injection cycle (*Refresh*
618 *Fraction*) was determined. This calibration requires the filling of all eight reactors with a
619 fluorescent reference solution. In this case, a purified FITC-dextran solution (25 µM) was used.
620 Subsequently, the reactors are diluted 10 times with milliQ water. By measuring the decrease in
621 fluorescence per dilution cycle for each reactor, the volume of fluid displaced during a single
622 injection cycle was determined. Within the LabVIEW software, this value (the *Refresh Ratio*) was
623 recorded for use during the IVTT experiment. Crucially, to account for variations in the flow rate
624 across the device, as well as discrepancies in the individual reactor volumes, the *Refresh Ratio* is
625 determined and stored for each individual reactor. The sequence of filling and diluting the
626 reactors was conducted automatically using the '*Perform Calibration*' program which forms part
627 of the LabVIEW software. The results of the calibration experiment are shown in **Figure 8**.

628 The most complex pre-programmed process executes a long-duration IVTT experiment, allowing
629 users to initiate the experiment and subsequently allow it to operate unattended until
630 completion. Throughout the experiment, reactors 1 and 5 were used as blanks, with only water
631 being added to the reactors during dilutions. Reactors 2 and 6 were utilised as negative controls
632 and contained only IVTT reaction solution and milliQ water. The remaining reactors (3, 4, 7, and
633 8) contained the IVTT reaction solutions and 2.5 nM of linear DNA coding for the deGFP gene.
634 Initialisation of the reactors is achieved by fully filling all the reactors (excluding 1 and 5) with the
635 IVTT reaction solution, before 25 % of the reactor volume was displaced with milliQ water.
636 Hereafter, the periodic injection of reagents into the reactors was initiated. The experiment was
637 conducted such that new reagents were injected into the reactors every 14.7 minutes, with 30 %
638 of the reactor volume being displaced during each dilution cycle. The composition of each
639 injection was such that 75 % of the injected fluid comprised fresh IVTT solution, whilst the
640 remaining 25 % consisted of either DNA or milliQ water. Following each injection of new reagents
641 the reactors were continuously mixed, after which a fluorescence image of each reactor was
642 recorded using the microscope. The reaction was subsequently allowed to run continuously for
643 68 cycles, resulting in an experimental duration of 16.5 h. The results of this experiment are given
644 in **Figure 9**.

645

646 When performing prolonged IVTT experiments, there are two main causes for the failure of a
647 reaction; the introduction of air into the microfluidic device or the degradation of the IVTT
648 reaction solution. The occurrence of air within the microfluidic device is most often the direct
649 result of small air bubbles existing in the inflow solutions, which are subsequently injected into
650 the microfluidic device. Upon entering the device, the presence of air inhibits the proper flow of
651 fluids, whereby the reactions are no longer periodically refreshed leading to the formation of
652 batch reactions within the reactor rings. In some cases, the air is slowly removed from the device
653 by the repeated flushing of reagents, after which the reaction continues as intended (as shown
654 in **Figure 9**). In other cases the air remains trapped, and can only be removed by aborting the

655 experiment and subsequently applying continuous (high) pressure to the flow layer of the
656 microfluidic device, analogous to the filling process described in Section 6.1.3 of the protocols.
657 During our experiments the cell lysate is stored in PTFE tubing on a Peltier element cooled to 4
658 °C. Both measures aid in limiting the degradation of the IVTT reaction solution over time, with
659 the inert PTFE tubing ensuring limited interaction between the tubing and the reaction solution
660 and the cold temperatures preserving the functional (bio)molecular componentry required to
661 perform IVTT. Should degradation of the reaction solution occur – as the result of insufficient
662 cooling or undesired interactions between the reaction solution and the storage environment –
663 then this will exhibit itself experimentally as a gradual reduction of protein expression over time.
664 Once degraded, the IVTT reaction solution cannot be recovered and a new experiment should be
665 prepared.

666

667 Figures

668

669 **Figure 1. The hardware setup required to perform continuous IVTT reactions.** A) Schematic of
670 the hardware setup. B) Photograph of the setup used throughout this manuscript. The
671 implementation of a multilayer microfluidic device for continuous IVTT reactions requires an
672 extensive hardware setup to regulate flow pressure, actuate control channels, heat and cool
673 reactions and reagents, store fluids, and image the device during experiments. Experiments are
674 performed at temperatures of 30 °C, which is achieved by placing the microscope within an
675 incubator set to this temperature. To prevent deterioration of the IVTT reaction solution, it is
676 stored within PTFE tubing coiled over the cold face of a Peltier element. The temperature of the
677 Peltier element is set to 4 °C, with a water cooler and water block being used to maintain this
678 temperature. Reagents which do not require cooling, are stored in fluid reservoirs outside of the
679 microscope incubator. Constant pressure is applied to these reservoirs by a computer controlled
680 pressure regulator. In this manner, the fluids are forced through the outlet tubing of the
681 reservoirs, which connect directly to the inflow channels of the microfluidic device. Each of the
682 control channels of the microfluidic device is connected to a pneumatic valve. The entire valve
683 array is under constant pressure. Opening the valve, allows for pressurisation of the fluid within
684 the tubing connecting the pneumatic valve to the control channel of the microfluidic device, thus
685 opening and closing the PDMS membranes found within the microfluidic device. The pneumatic
686 valves are opened and closed via a LabVIEW interface which commands a WAGO-controller (not
687 shown) to open and close specific pneumatic valves. Figure adapted from Yelleswarapu *et al.*³⁷.

688

689 **Figure 2. Overview of the pneumatic valve setup and control channel connection.** An 8-valve
690 array is shown with three control channel connections fitted to valves 1, 2, and 3. Compressed air
691 can be supplied to the valve array via 1/4" tubing. For the actuations of control channels two
692 pressures are used: 1 bar for the lower pressure control channels (1, 2, and 3) and 3 bar for the
693 higher pressure control channels (9 through 30, not shown here). The tygon tubing can be filled
694 with milliQ water and inserted into one of the control channel inlets using a stainless steel
695 connector pin.

696

697 **Figure 3. Overview of the commercial flow pressure regulator and reservoir system.** A
698 commercially available pressure regulator is used to inject fluids into the flow layer of the

699 multilayer microfluidic device. Connecting the pressure controller to a computer allows for
700 modulation of the pressure used to perform the fluid injections. Reagents can be stored in a fluid
701 reservoir, which is directly connected to the pressure regulator. The application of pressure to the
702 reservoir forces the fluid out of the reservoir via the outlet tubing. This outlet tubing can be
703 connected directly to one of the fluid inlets of the microfluidic device using a stainless steel
704 connector pin. In the event that the reagent volume is unable to reach the fluid reservoir, the
705 tygon outlet tubing acts as a reservoir for the reagent.

706

707 **Figure 4. Overview of the cooling system used to cool reaction reagents.** A) Isolated cooling
708 setup and B) Cooling setup placed within the microscope and connected to the microfluidic
709 device. A Peltier element is used to cool the IVTT reaction solution prior to injection into the
710 microfluidic device. The reagent is stored within PTFE tubing coiled over the cold-face of the
711 Peltier element. A length of PEEK tubing is used to transfer the cooled fluid to the microfluidic
712 device, with the small internal diameter (0.005") minimising the reagent volume no longer being
713 cooled. Alongside the coiled PTFE tubing, a thermistor is placed, allowing for real-time
714 temperature monitoring on the surface of the Peltier element. The voltage applied to the Peltier
715 is set such that the surface temperature of the Peltier remains between 0 °C and 4 °C. To remove
716 excess heat produced by the Peltier element, the hot-face of the Peltier is placed against a water
717 cooled block, with the addition of thermal paste ensuring optimal heat transfer between the two
718 faces.

719

720 **Figure 5. Overview of the microfluidic device design.** The microfluidic flow reactor for continuous
721 IVTT reactions consists of eight reactor rings, each with a volume of 10.7 nL. Nine inlets allow for
722 the inflow of nine unique reaction solutions into the device. 24 control channels regulate the flow
723 of fluids within the device. Control channels 9 through 14 form a multiplexer. These control
724 channels should be pressurised at all times to inhibit fluid flow into the device. Depressurisation
725 of two control channels simultaneously allows for the inflow of a single reagent. Control channels
726 15, 16, and 17 are used to peristaltically pump the reagents into the device in a controlled manner.
727 Control channels 18 through 25 each control the inlet of one of the eight reactors found within
728 the device. Control channel 26 can close the flush channel, thus forcing fluid into the reactors.
729 Control channel 27 aids in the homogeneous filling of the reactors. Control channels 28 and 29
730 regulate the ring reactor outlets and the only device outlet respectively. Finally, control channels
731 1, 2, and 3 are used to peristaltically pump the fluid within the ring reactors, resulting in mixing
732 of the reagents. The design of this microfluidic device and the figure are both adapted from
733 Neiderholtmeyer *et al.*²⁹.

734

735 **Figure 6. LabVIEW interface used to control microfluidic device.** Throughout this research, a
736 custom LabVIEW interface has been used to control the flow of fluids within the microfluidic
737 devices. The interface allows users to individually actuate each of the control channels (numbered
738 1-3 and 9-29), or to execute elaborate protocols resulting in the flushing and loading of reagents,
739 the calibration of the microfluidic device, and the execution of experiments.

740

741 **Figure 7. Membrane based valve within the microfluidic device.** A) Flow channel within the
742 microfluidic device. Two control channels can be seen in the background. These channels are not

743 pressurised and as such the valves are open (fluid can flow). B) The two control channels
744 intersecting the flow layer channels have been pressurised, closing the valves (i.e. fluid flow is
745 impeded). Upon pressurisation of the control channels, the thin PDMS membrane separating the
746 flow and control layer channels is deflected upwards (the control layer lies beneath the flow layer)
747 which closes the flow layer channel. The rounding of the flow layer channel is critical in ensuring
748 that the deflected membrane fully closes the flow channel.

749

750 **Figure 8. Results of a calibration experiment.** During a calibration experiment, the reactors are
751 filled with a fluorophore (25 µM FITC-Dextran) after which the fluorescence intensity is recorded.
752 Subsequently, a series of dilutions follow, where a set number of inflow steps (15) are used to
753 inject milliQ water into the reactors. After each dilution, the reagents are mixed and the
754 fluorescence is measured. The decrease in the fluorescence intensity per dilution reveals the
755 volume of the reactor ring displaced for the set number of inflow steps; a value termed the
756 *Refresh Ratio*. A) The average intensity and standard deviation of all eight reactors is shown in
757 red, with the individual intensity traces shown in grey. B) The average *Refresh Ratio* and standard
758 deviation is shown for each dilution step in red. The individual *Refresh Ratios* of each individual
759 reactor are shown in grey. It can be seen that seven of the eight reactors show very similar
760 behaviour, however one reactor shows fluctuations in the *Refresh Ratio* after the seventh dilution
761 cycle. This highlights the need for unique *Refresh Ratios* for each of the reactors, as opposed to
762 using an average *Refresh Ratio* for the injection of reagents into the reactors.

763

764 **Figure 9. Results of an IVTT experiment expressing the deGFP protein.** A prolonged IVTT reaction
765 was initiated such that 30 % of the reactor volume is displaced every 14.6 minutes. The reaction
766 was allowed to run for over 16 hours before being terminated. Two reactors of the microfluidic
767 device were used as blanks, with only milliQ water being flown through the reactors throughout
768 the experiment (reactors 1 and 5). All the other reactors comprised 75 % IVTT reaction solution
769 and 25 % of either milliQ water (reactors 2 and 6) or 2.5 nM linear DNA templates coding for the
770 expression of deGFP (reactors 3, 4, 7, and 8). In all four reactors where DNA was added, there is
771 clear deGFP expression. Three of the four reactors provide similar fluorescence intensity, with
772 one reactor displaying lower fluorescence signal. This could be caused by a disparity in flow
773 resulting in less DNA entering the reactor, or due to variations in the reactor dimensions. After 14
774 hours, a sudden increase is seen in the signal of the reactors containing DNA. This is caused by an
775 air bubble entering the flow layer of the microfluidic device, presumably originating from one of
776 the inflow solutions. The trapping of air in the microfluidic device significantly limits the flow of
777 fluids through the channels, whereby no fresh reagents can be added to or removed from the
778 reactors until the air has passed. Upon resumption of flow, the experiment returns to its previous
779 fluorescence intensity.

780

781 **Discussion (3-6 Paragraphs)**

782 A PDMS-based multilayer microfluidic device has been presented, and its capability to sustain
783 IVTT reactions for prolonged periods of time has been demonstrated. Although well-suited for
784 this specific example, this technology can conceivably be used for numerous other applications.
785 The additional control over fluid flow – paired with the ability to continuously replenish reaction
786 reagents whilst removing (by)products – is ideal for continuous synthesis reactions, the

787 investigation of various dynamic behaviours, and the simultaneous conduction of multiple
788 variations of a single reaction.

789
790 Despite the relatively straightforward fabrication process of PDMS based devices, the use thereof
791 requires an extensive hardware setup. Comprising valve arrays, pressure regulators, pressure
792 pumps, incubators, and cooling units, the transition from fabrication to use is not elementary,
793 and requires a significant initial investment. In addition, the ability to consistently set-up and
794 perform successful experiments with these devices requires a significant time-investment; a
795 point which this manuscript aims to address. However, once in place, the entire setup can be
796 modified for a range of purposes. Furthermore, the hardware setup comprises numerous
797 modular elements, each of which can be expanded to allow more complex microfluidic device
798 designs to be employed. Additionally, the modular design enables the replacement of hardware
799 components by similarly functioning alternatives, such that users are not limited to the specific
800 setup described here^{38,39}.

801
802 Variability between individual devices, and in the external conditions (such as pressure
803 fluctuations) can result in inaccuracies when performing experiments using these devices. To
804 address this issue, a calibration of the system should be performed prior to each experiment,
805 providing a unique *Refresh Ratio* for each of the reactors. Whilst the calibration addresses the
806 device-to-device and experiment-to-experiment variations, it is a time consuming process and
807 not flawless. Fluids with differing viscosities will not flow with the same rate when exposed to
808 identical pressure, and as such performing the calibration with multiple reagents may not yield
809 identical *Refresh Ratios*. This effect is attenuated by utilising three control channels to
810 peristaltically pump the reagents into the microfluidic device, as opposed to regulating the flow
811 by varying the supplied pressure only. As a last resort in cases where the disparity in viscosity is
812 very large, a unique *Refresh Ratio* can be implemented for each individual reagent by performing
813 multiple calibration experiments.

814
815 The use of a peristaltic pump to inject reagents into the microfluidic device attenuates the effects
816 of using solutions with varying viscosities, however it also creates a secondary problem. Using
817 discrete steps to pump fluids into the microfluidic device, means that the resolution of injections
818 into a single reactor, is limited by the volume injected when performing a single pump cycle.
819 Within our research this value – determined during the calibration – is approximately equal to 1
820 %, indicating that a single pump cycle displaces approximately 1 % of the reactor volume (about
821 0.1 nL). As such, displacing 30 % of the reactor volume requires the execution of 30 pump cycles,
822 with 23 pump cycles of the IVTT reaction solution being added, and only 7 pump cycles of DNA
823 or milliQ water being added. Although sufficient for our research, alternative experimental
824 protocols may encounter problems when attempting to add larger numbers of unique reagents,
825 use a lower *Refresh Fraction*, or add smaller volumes of a single reagent to a reactor. In such
826 cases, the microfluidic device design can be adapted to provide reactors with a larger volume. An
827 example of such is reported in Niederholtmeyer *et al.*²⁹.

828
829 Crucially, the device outlined within this manuscript allows reactions to be sustained for
830 prolonged durations resulting in steady-state transcription and translation rates. By periodically

831 injecting new reagents into the reactors – and removing reaction (by)products – the reactions
832 are sustained and complex dynamic behaviours can be monitored. In this way, a platform has
833 been created that – to some extent – mimics the cellular environment. Furthermore, this
834 platform enables the exploration of the system dynamics, by adapting the period between
835 injections and the specific composition of the injections. As a result, these multilayer microfluidic
836 devices are a powerful tool for the characterisation and optimisation of novel synthetic networks
837 which display complex dynamic behaviour.

838

839 **Acknowledgements**

840 This work was supported by the European Research Council, ERC (project n. 677313 BioCircuit)
841 an NWO-VIDI grant from the Netherlands Organization for Scientific Research (NWO,
842 723.016.003), funding from the Ministry of Education, Culture and Science (Gravity programs,
843 024.001.035 & 024.003.013)

844

845 **Disclosures**

846 The authors declare that they have no competing financial interests.

847

848 **Table of Materials / Equipment**

849 See attached Excel sheet.

850

851 **References**

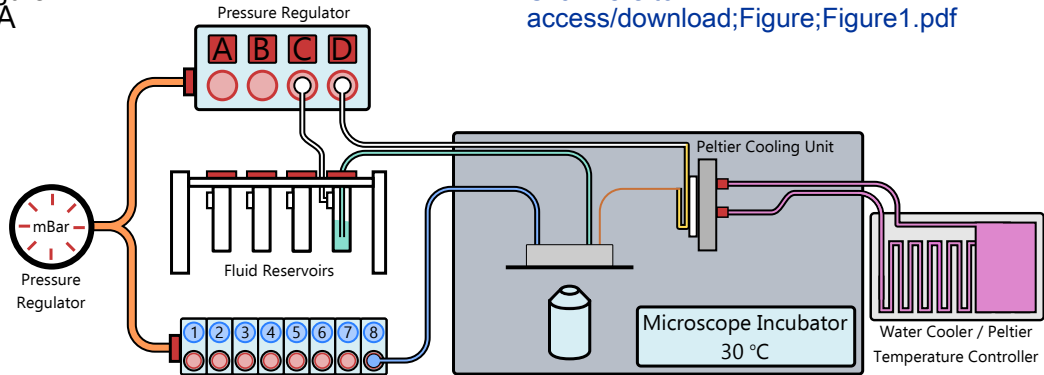
- 852 1. van Roekel, H. W. H. *et al.* Programmable chemical reaction networks: emulating
853 regulatory functions in living cells using a bottom-up approach. *Chem. Soc. Rev.* **44**,
854 7465–7483 (2015).
- 855 2. Yutaka Hori, Chaitanya Kantak, R. M. M. and A. R. A. Cell-free extract based optimization
856 of biomolecular circuits with droplet microfluidics. *Lab Chip* (2017).
857 doi:10.1039/C7LC00552K
- 858 3. Del Vecchio, D. & Sontag, E. D. Dynamics and control of synthetic bio-molecular
859 networks. 1577–1588 (2007).
- 860 4. Purnick, P. E. M. & Weiss, R. The second wave of synthetic biology: from modules to
861 systems. *Nat. Rev. Mol. Cell Biol.* **10**, 410–422 (2009).
- 862 5. Padirac, A., Fujii, T. & Rondelez, Y. Bottom-up construction of in vitro switchable
863 memories. *Proc. Natl. Acad. Sci.* **109**, E3212–E3220 (2012).
- 864 6. Guido, N. J. *et al.* A bottom-up approach to gene regulation. *Nature* **439**, 856–860 (2006).
- 865 7. Genot, A. J., Fujii, T. & Rondelez, Y. In vitro regulatory models for systems biology.
866 *Biotechnol. Adv.* **31**, 789–796 (2013).
- 867 8. Elowitz, M. B. & Leibler, S. A synthetic oscillatory network of transcriptional regulators.
868 *Nature* **403**, 335–338 (2000).
- 869 9. Gardner, T. S., Cantor, C. R. & Collins, J. J. Construction of a genetic toggle switch in
870 *Escherichia coli*. *Nature* **403**, 339–342 (2000).
- 871 10. Montagne, K., Plasson, R., Sakai, Y., Fujii, T. & Rondelez, Y. Programming an in vitro DNA
872 oscillator using a molecular networking strategy. *Mol. Syst. Biol.* **7**, 466–466 (2014).
- 873 11. Khalil, A. S. & Collins, J. J. Synthetic biology: applications come of age. *Nat. Rev. Genet.*
874 **11**, 367–379 (2010).

- 875 12. Hockenberry, A. J. & Jewett, M. C. Synthetic in vitro circuits. *Curr. Opin. Chem. Biol.* **16**,
876 253–259 (2012).
- 877 13. Vecchio, D. Del. Modularity, context-dependence, and insulation in engineered biological
878 circuits. *Trends Biotechnol.* **33**, 111–119 (2015).
- 879 14. Cardinale, S. & Arkin, A. P. Contextualizing context for synthetic biology - identifying
880 causes of failure of synthetic biological systems. *Biotechnol. J.* **7**, 856–866 (2012).
- 881 15. Venturelli, O. S. *et al.* Programming mRNA decay to modulate synthetic circuit resource
882 allocation. *Nat. Commun.* **8**, 1–11 (2017).
- 883 16. Scott, M., Mateescu, E. M., Zhang, Z. & Hwa, T. Interdependence of cell growth and gene
884 expression: origins and consequences. **330**, 1099–1103 (2010).
- 885 17. Borkowski, O., Ceroni, F., Stan, G. B. & Ellis, T. Overloaded and stressed: whole-cell
886 considerations for bacterial synthetic biology. *Curr. Opin. Microbiol.* **33**, 123–130 (2016).
- 887 18. Liao, C., Blanchard, A. E. & Lu, T. An integrative circuit–host modelling framework for
888 predicting synthetic gene network behaviours. *Nat. Microbiol.* (2017).
889 doi:10.1038/s41564-017-0022-5
- 890 19. Noireaux, V., Bar-ziv, R. & Libchaber, A. Principles of cell-free genetic circuit assembly.
891 **2003**, (2003).
- 892 20. Nishikawa, K. & Ueda, T. Cell-free translation reconstituted with purified components.
893 **19**, 751–755 (2001).
- 894 21. Oberholzer, T., Nierhaus, K. H. & Luisi, P. L. Protein expression in liposomes. *Biochem.
895 Biophys. Res. Commun.* **261**, 238–241 (1999).
- 896 22. Hughes, R. A. & Ellington, A. D. Synthetic DNA Synthesis and Assembly : Putting the
897 Synthetic in Synthetic Biology. (2017).
- 898 23. Garamella, J., Marshall, R., Rustad, M. & Noireaux, V. The all E. coli TX-TL toolbox 2.0: A
899 platform for cell-free synthetic biology. *ACS Synth. Biol.* **5**, 344–355 (2016).
- 900 24. Takahashi, M. K. *et al.* Characterizing and prototyping genetic networks with cell-free
901 transcription-translation reactions. *Methods* **86**, 60–72 (2015).
- 902 25. Lee, J. W. *et al.* Creating Single-Copy Genetic Circuits. *Mol. Cell* **63**, 329–336 (2016).
- 903 26. Gibson, D. G. *et al.* Complete chemical synthesis, assembly, and cloning of a mycoplasma
904 genitalium genome. *Science* **319**, 1215–1220 (2008).
- 905 27. Sun, Z. Z., Yeung, E., Hayes, C. A., Noireaux, V. & Murray, R. M. Linear DNA for rapid
906 prototyping of synthetic biological circuits in an Escherichia coli based TX-TL cell-free
907 system. *ACS Synth. Biol.* **3**, 387–397 (2014).
- 908 28. Georgi, V. *et al.* On-chip automation of cell-free protein synthesis: new opportunities due
909 to a novel reaction mode. *Lab Chip* **16**, 269–281 (2016).
- 910 29. Niederholtmeyer, H., Stepanova, V. & Maerkl, S. J. Implementation of cell-free biological
911 networks at steady state. *Proc. Natl. Acad. Sci.* **110**, 15985–15990 (2013).
- 912 30. A. S. Spirin, V. I. Baranov, L. A. Ryabova, S. Y. Ovodov, and Y. B. A. A Continuous Cell-Free
913 Translation System Capable of Producing Polypeptides in High Yield. *Science* **242**, 1162–
914 1164 (1988).
- 915 31. Karzbrun, E., Tayar, A. M., Noireaux, V. & Bar-Ziv, R. H. Programmable on-chip DNA
916 compartments as artificial cells. *Science* **345**, 829–832 (2014).
- 917 32. Khnouf, R., Beebe, D. J. & Fan, Z. H. Cell-free protein expression in a microchannel array
918 with passive pumping. *Lab Chip* **9**, 56–61 (2009).

- 919 33. Siuti, P., Retterer, S. T. & Doktycz, M. J. Continuous protein production in nanoporous,
920 picolitre volume containers. *Lab Chip* **11**, 3523–3529 (2011).
- 921 34. Niederholtmeyer, H. *et al.* Rapid cell-free forward engineering of novel genetic ring
922 oscillators. *Elife* **4**, 1–18 (2015).
- 923 35. Galas, J., Haghiri-Gosnet, A.-M. & Estévez-Torres, A. A nanoliter-scale open chemical
924 reactor. *Lab Chip* **13**, 415–423 (2013).
- 925 36. Unger, M. A., Chou, H., Thorsen, T., Scherer, A. & Quake, S. R. Monolithic microfabricated
926 valves and pumps by multilayer soft lithography. **288**, 113–117 (2000).
- 927 37. Yelleswarapu, M. *et al.* Sigma factor-mediated tuning of bacterial cell-free synthetic
928 genetic oscillators. *ACS Synth. Biol.* **7**, acssynbio.8b00300 (2018).
- 929 38. Brower, K. *et al.* An open-source, programmable pneumatic setup for operation and
930 automated control of single- and multi-layer microfluidic devices. *HardwareX* **3**, 117–134
931 (2018).
- 932 39. White, J. A. & Streets, A. M. Controller for microfluidic large-scale integration. *HardwareX*
933 **3**, 135–145 (2018).
- 934
- 935
- 936
- 937
- 938

REVIEWER PDF

Figure 1
A



Click here to access/download;Figure;Figure1.pdf

B

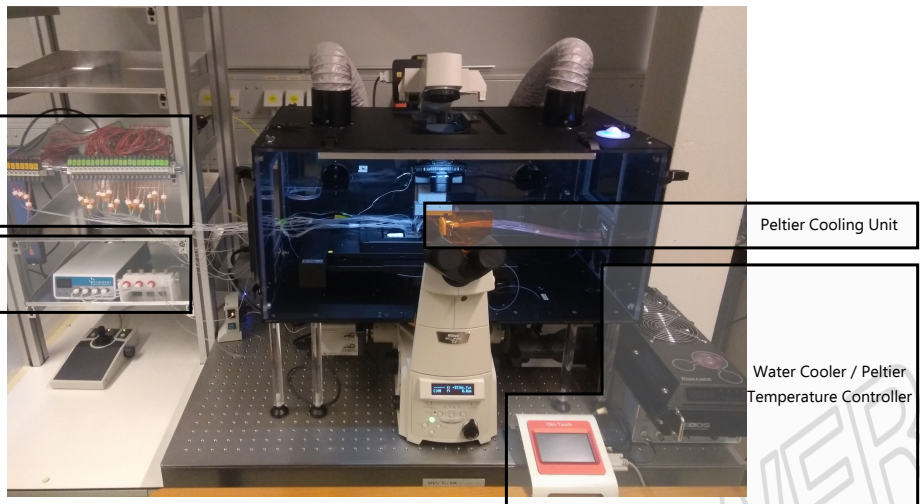
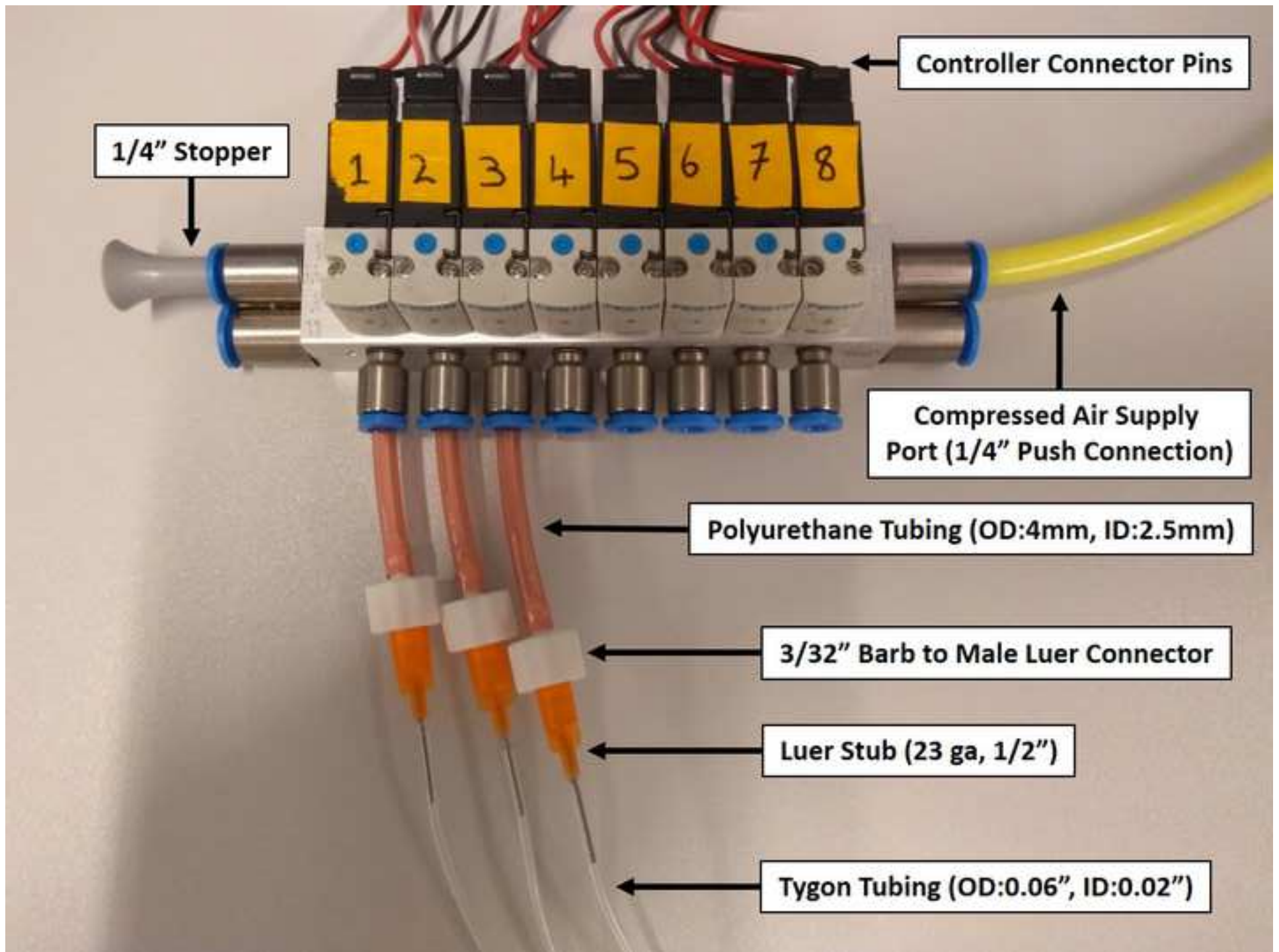


Figure 2

[Click here to access/download;Figure;Figure2.jpg](#)



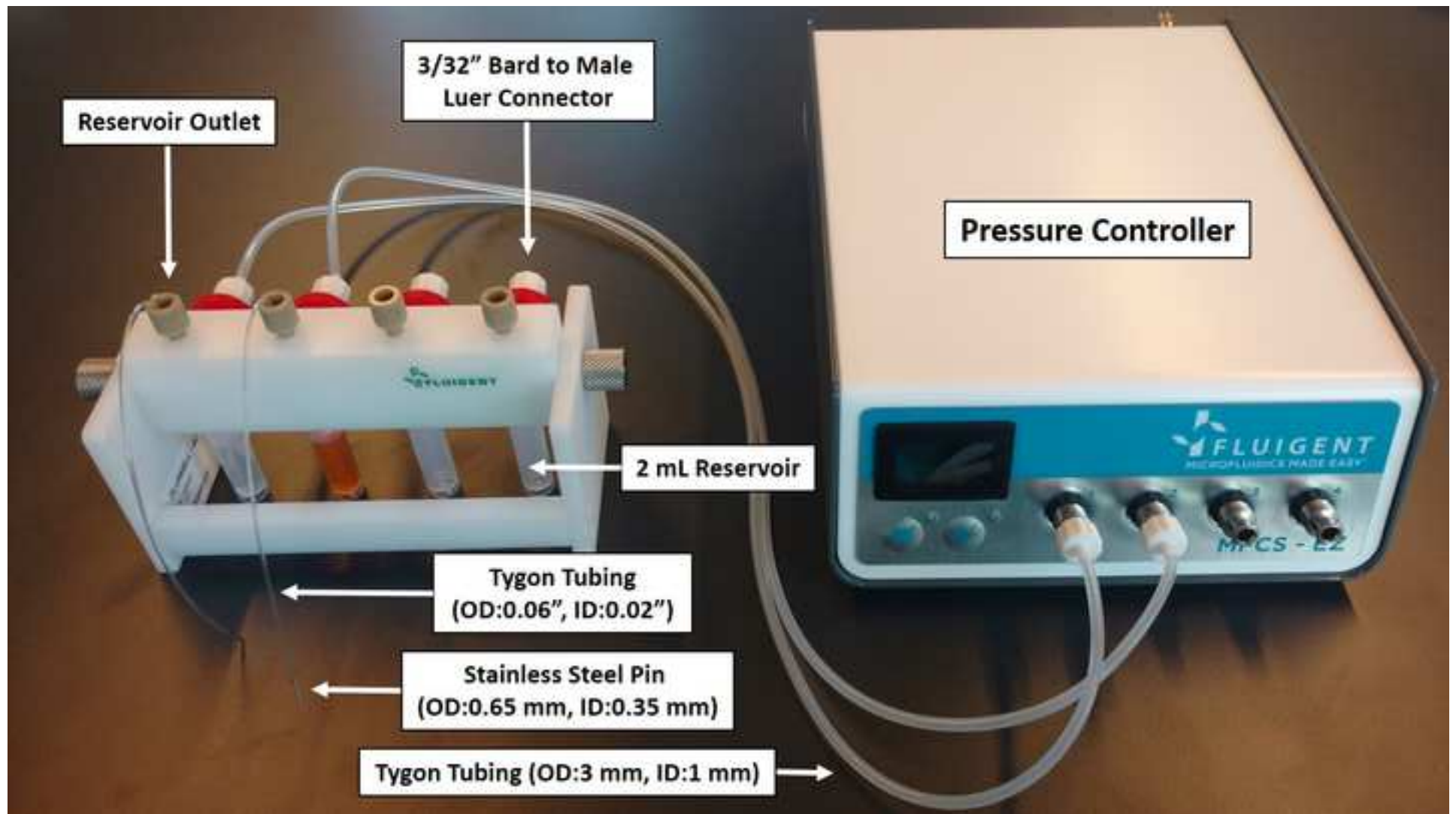


Figure 4

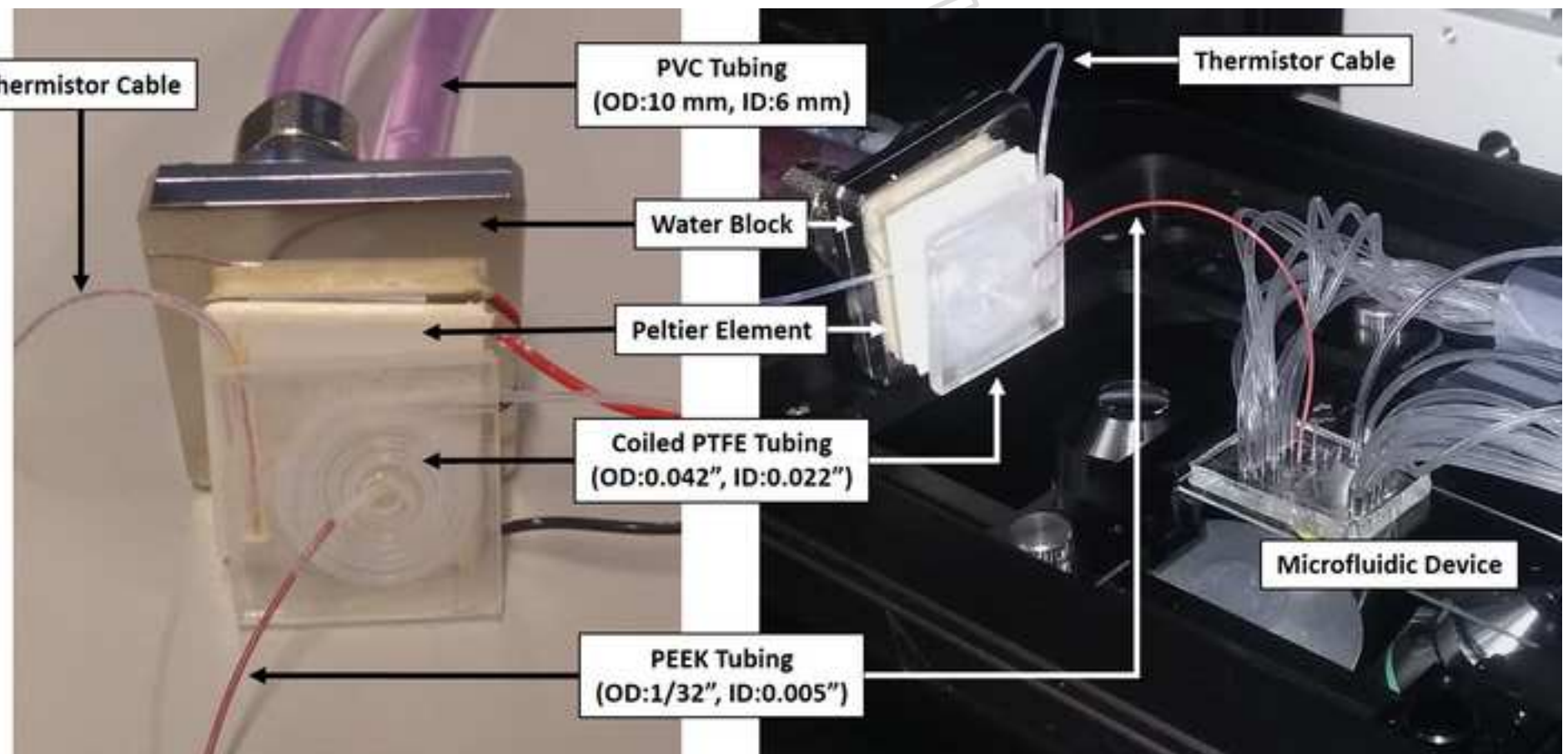
[Click here to access/download;Figure;Figure4.jpg](#)

Figure 5

[Click here to access/download;Figure;Figure5.pdf](#)

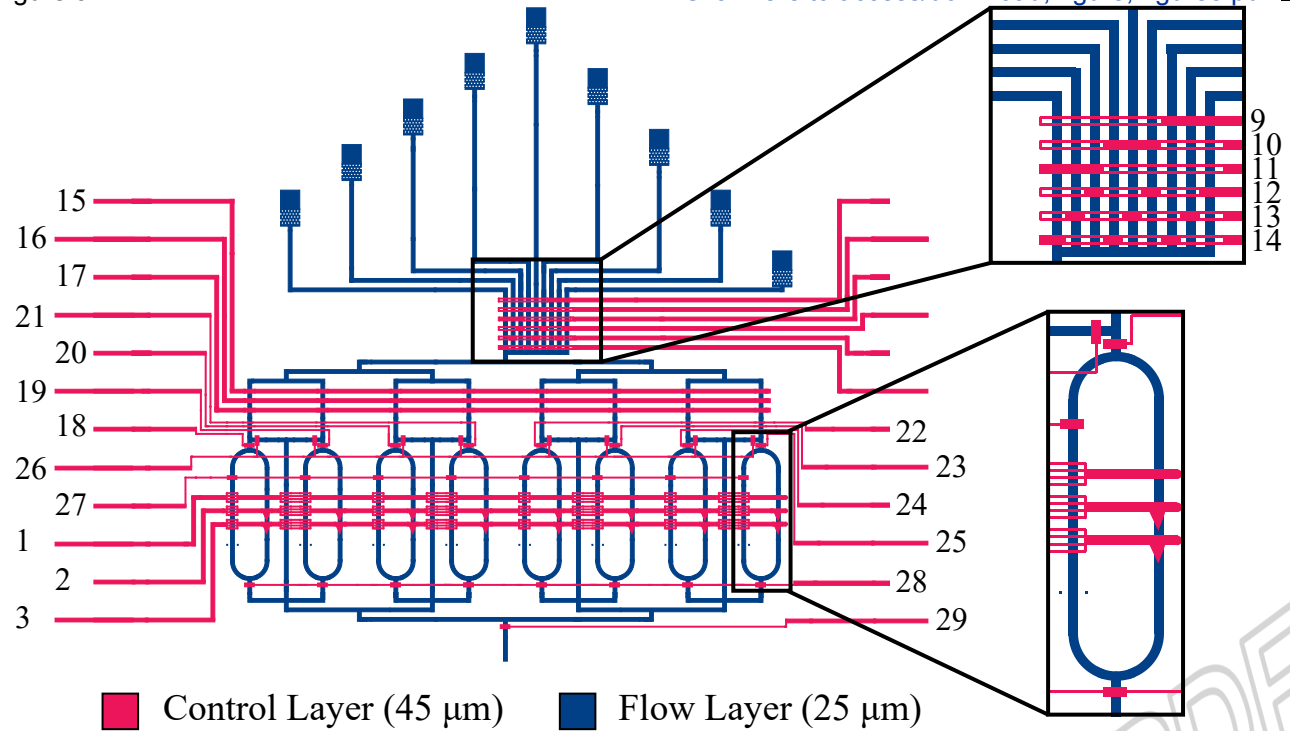


Figure 6

[Click here to access/download;Figure;Figure6.jpg](#)

<p>Address: 192.168.1.100 Port: 502 Timeout (ms): 25</p> <p>Bytes Written (Per Command): 0 Bytes Written (Total): 0</p> <p>Line Pressure Control channels 4-8 Should Remain Unused. If Additional Air Lines Are Required, The Valves Can Be Found Under This Tab.</p>	<p>4x Filled Control Lines</p> <p>1 2</p> <p>3</p>	<p>Microfluidic</p> <p>4 12</p> <p>5 10</p> <p>6 11</p> <p>7 14</p>	<p>Micro Speed Regulators</p> <p>8 16</p> <p>9 17</p>	<p>Valve Control</p> <p>10 22</p> <p>11 23</p> <p>12 24</p> <p>13 25</p> <p>14 26</p>	<p>Micro</p> <p>15 27</p> <p>16 28</p> <p>17 29</p>	<p>Experimental Sequence</p> <p>Perform Experiments</p> <p>Channel Selection Set Dilution RR</p> <p>Dilution Buffer Dilution Buffer RR 1 0.25 Fluorophore Fluorophore RR F1 0 F2 0.88 F3 0.71</p> <p>EPR for Multiple DNA Concentration</p> <p>DNA Channel DNA_High RR 1 0.25</p> <p>Refill Processors</p> <p>Mixing Processor</p> <p>Number Of Mix Cycles: 1 Interval (min): 1 Mix Chamber</p> <p>Cycles completed: 0 Time since start (sec): 0</p> <p>Flush</p> <p>Flush Channel: 1 Flush Fast Flush Slow</p> <p>Progress P: 0 Progress: 0</p> <p>Load</p> <p>Load Channel: 1 Load Full Load 20%</p> <p>Ring 1 Ring 2 Ring 3 Ring 4 Ring 5 Ring 6 Ring 7 Ring 8</p> <p>Progress: 0</p> <p>Perform Initial Calibration</p> <p>Refresh Ratio: 8 Duration (min): 0 Running Calibration: Running</p> <p>Number of Mixing Cycles: 4 Time between Mixing Cycles: 0</p> <p>Number of Dilution Steps: 10 Dilution Buffer Channel: 12 Fluorophore Channel: 1 Number of Inflow Steps: 13</p> <p>Refill fraction (%): 10 Number of Mixing Cycles Initialization: 4 Time between Mixing Cycles Initialization: 3 Number of Dilution Cycles: 120 Running Experiments: Running Time since start (sec): 0</p>
---	--	--	--	--	--	---

Figure 7

[Click here to access/download;Figure;Figure7.jpg](#) ↗

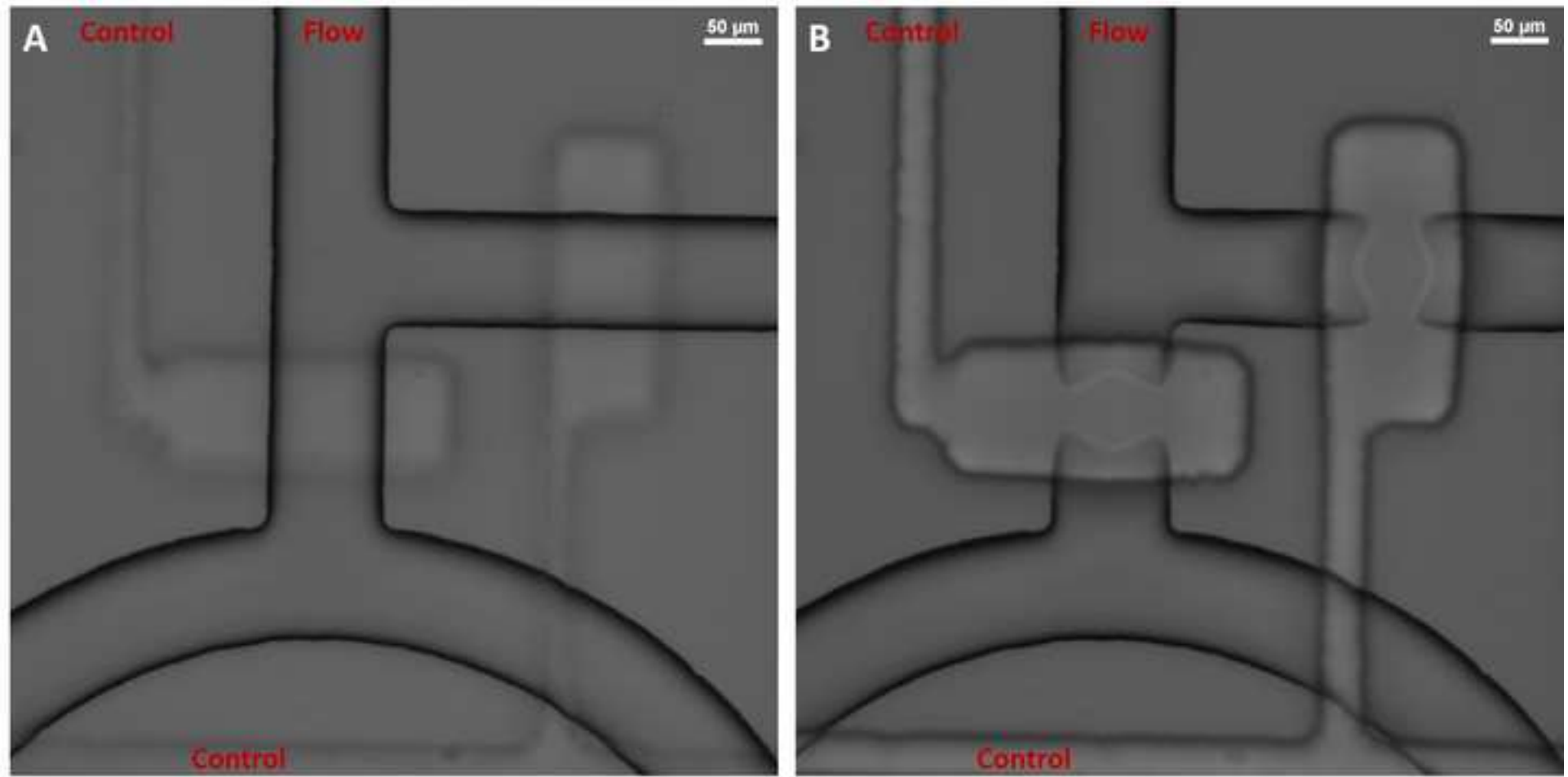


Figure 8

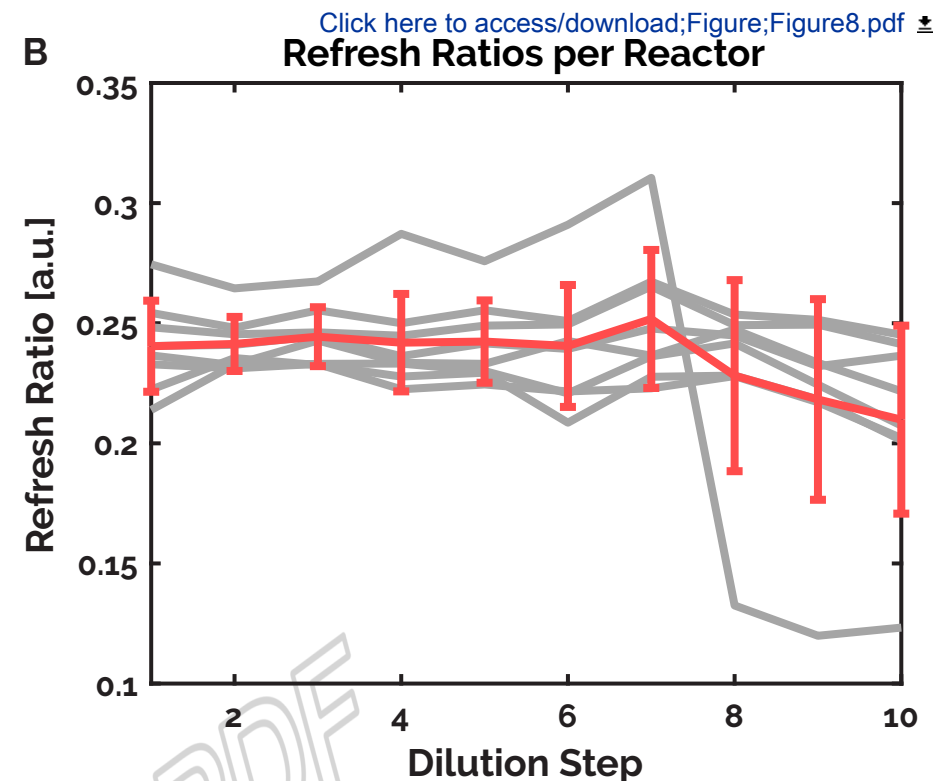
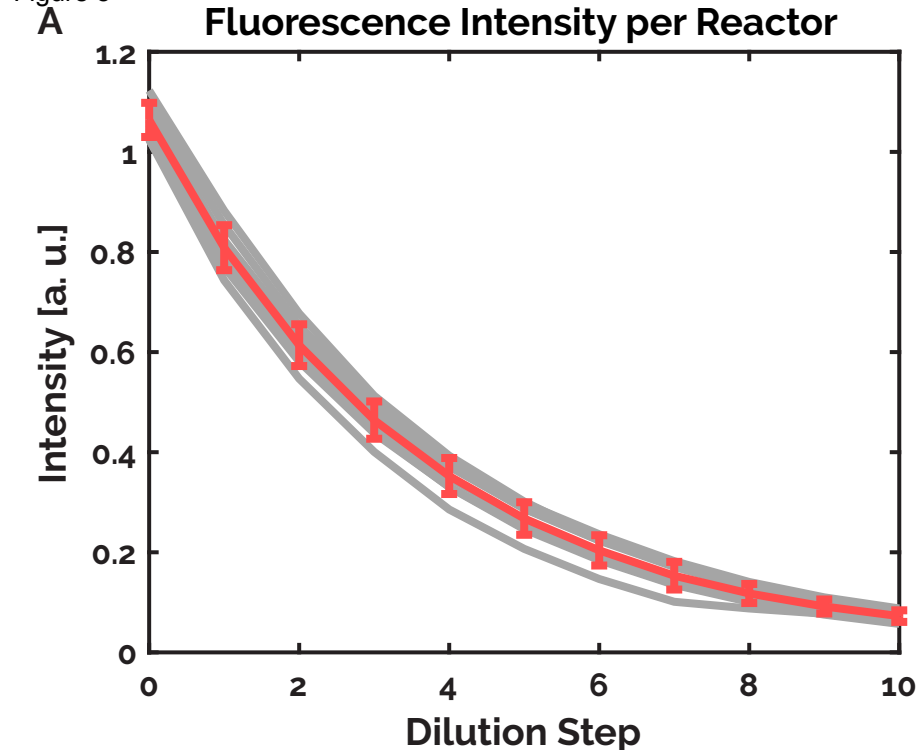
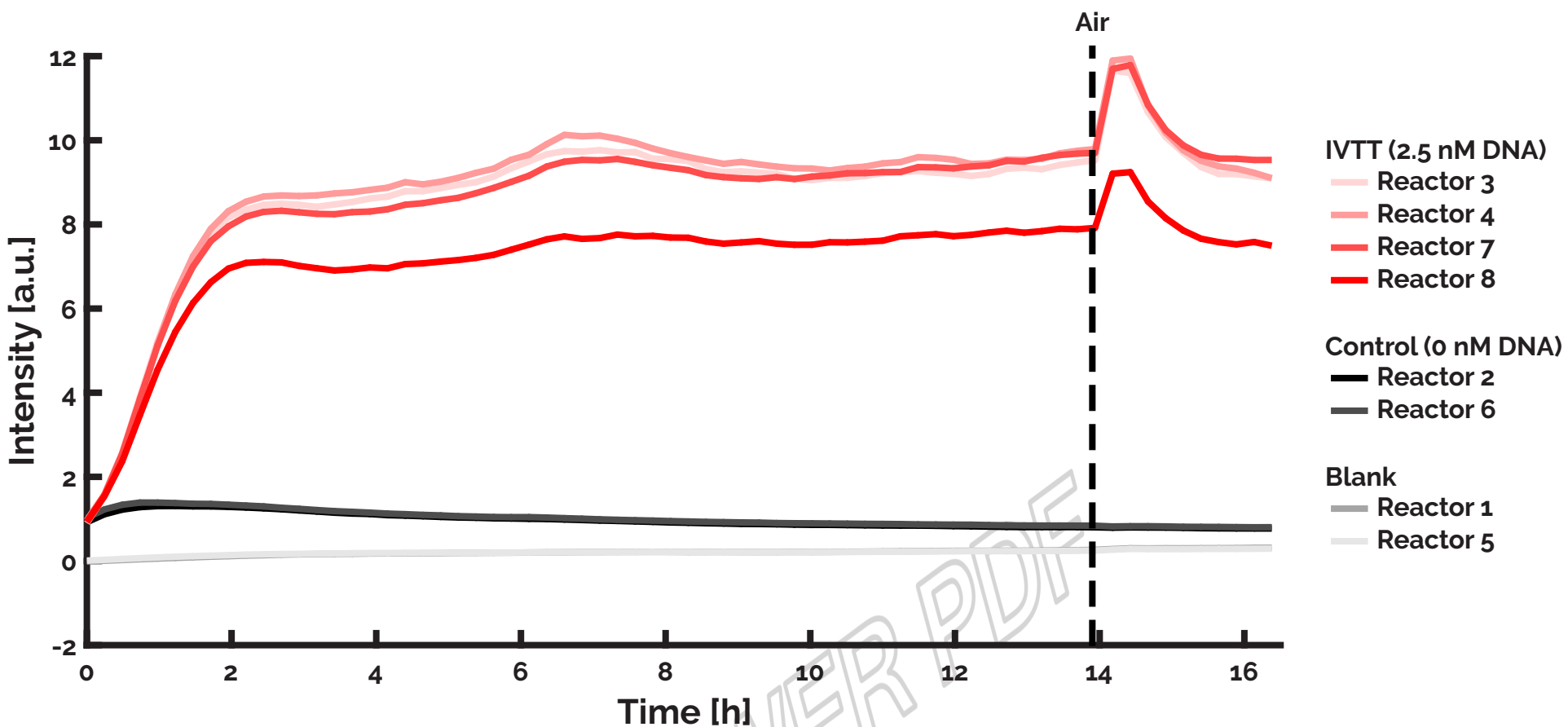


Figure 9

Fluorescence Intensity of deGFP Expression

[Click here to access/download;Figure;Figure9.pdf](#)

Name of Material/ Equipment	Company	Catalog Number
Reagents		
mr Dev 600	Microresist Technology GmbH (Berlin, Germany)	-
AZ 40 XT	Merck KGaA (Darmstadt, Germany)	-
SU-8 3050	Microchem Corp. (Newton, MA)	-
AZ 726 MIF Developer	Merck KGaA (Darmstadt, Germany)	-
Acetone	VWR	20063.365
Isopropanol	Merck KGaA (Darmstadt, Germany)	109634
Sylgard 184 Elastomer Kit (PDMS)	The Dow Chemical Company	01317318
Silicon wafers	Silicon Materials	-
Microscope slides	VWR	ECN 631-1550
trichloro(1H,1H,2H,2H- perfluoroctyl)silane	Sigma-Aldrich	448931-10G
Equipment		
Photomask Design	Maerkli Lab, EPFL de Greef Lab, Eindhoven	https://zenodo.org/record/886937#.XBzpA8-2nOQ
LabVIEW Software	University of Technology de Greef Lab, Eindhoven	https://github.com/tfadgref/Microfluidic-Device-Control-Software
Matlab Software	University of Technology Laurell Technologies	https://github.com/tfadgref/Microfluidic-Device-Control-Software
Spin coater	Corporation	WS-650MZ-23NPPB
Orbital shaker	Cole Parmer	EW-513000-05
Hot plate	Torrey Pines Scientific	HP61
UV exposure system	ABM, USA	-

	Advanced Radiation	
Hg short arc lamp	Corporation	-
Oven	Thermo Scientific	Heraeus T6P 50045757
PDMS puncher	SYNEO	Accu-Pucnh MP10
Punching pin	SYNEO	CR0320245N21R4
Microcamera	The Imaging Source	DMK 42AUC03
Camera lens	The Imaging Source	-
Single edge blades	GEM Scientific	-
Oxygen plasma ashер	Quorum Technologies	K1050X
Stereo microscope	Olympus Corporation	SZ61
Weighing scales	Sartorius	M-prove
Vacuum pump	Vacuumbrand GmbH	MD1C
Photomasks	CAD/Art Services, Inc.	-
Fluigent pressure system	Fluigent	MFCS-EZ
Fluid reservoirs	Fluigent	Fluiwell-4C
Pneumatic valve array	FESTO	-
Male Luer to barb connectors	Cole Parmer	45505-32
Luer stubs	Instech Laboratories, Inc.	LS23
Device connector pins	Unimed SA (Lausanne, Switzerland)	200.010-A
Ethernet Controller	WAGO Kontakttechnik GmbH	750-881
4 channel digital input/output module	WAGO Kontakttechnik GmbH	750-504
Controller end module	WAGO Kontakttechnik GmbH	750-600
Inverted microscope	Nikon Instruments	Eclipse Ti-E
Microscope camera	Hamamatsu Photonics	OrcaFlash4.0 V2 (C11440-22CU)
Compression fitting	Koolance, Inc.	FIT-V06X10
Water cooler	Koolance, Inc.	EX2-755
Power adapter	Koolance, Inc.	ADT-EX004S
Liquid coolant	Koolance, Inc.	LIQ-705CL-B
PVC Tubing	Koolance, Inc.	HOS-06CL

Water cooled cold plate block	Koolance, Inc.	PLT-UN40F
Peltier element	European Thermodynamics	APH-127-10-25-S
Peltier temperature controller	Warner Instruments	CL-100
	Saint-Gobain Performance	
Device connecting tubing	Plastics	AAD04103
Soft tubing	Fluigent	-
PTFE tubing	Cole Parmer	06417-21
Female bus connector	Encitech	DTCK15-DBS-K
Thermistor cable	Warner Instruments	TA-29
PEEK tubing	Trajan	1301005001-5F

REVIEWER PDF

Comments/Description

REVIEWER PDF

Near UV Exposure System, 350W

350W

OD: 0.032" (0.8128 mm), ID: 0.024" (0.6090 mm)

0 - 345 mbar

1x 22 valve array and 1x 8 valve array, Normally closed valves.

3/32" ID

AISI 304 tubing, 0.35mm ID, 0.65mm OD, 8mm L

8x

Fitting for tubing with 6mm ID and 10mm OD. 4x

110/220V AC Power Adapter

6 mm ID, 10 mm OD

0.02" ID, 0.06" OD, Tygon Tubing (ND-100-80)

Supplied with fluid reservoirs. (1 mm ID, 3mm OD)

#24 AWG Thin Wall PTFE

15 pole female bus connector

Cable with bead thermistor

0.005" ID, 1/32" OD, Red

REVIEWER PDF

[Click here to access/download](#)

Supplemental Coding Files

ConvertDesiredRefreshRatio.vi

[Click here to access/download](#)

Supplemental Coding Files

[ConvertDesiredRefreshRatioPerReactor.vi](#)

[Click here to access/download](#)

Supplemental Coding Files

[CurrentSwitchValues_GlobalVariable.vi](#)

Click here to access/download
Supplemental Coding Files
DeterminePingCommand.vi

[Click here to access/download](#)

Supplemental Coding Files

DetermineTimeSinceLastExecution.vi

Click here to access/download
Supplemental Coding Files
dummy_sender.exe

Click here to access/download
Supplemental Coding Files
dummy_stopper.exe

Click here to access/download
Supplemental Coding Files
MainInterface.vi

Click here to access/download
Supplemental Coding Files
SequenceSelector_Flush.vi

Click here to access/download
Supplemental Coding Files
SequenceSelector_Load.vi

Click here to access/download
Supplemental Coding Files
SequenceSelector_LoadAllChambers.vi

[Click here to access/download](#)

Supplemental Coding Files

[SequenceSelector_LoadPerReactor.vi](#)

Click here to access/download
Supplemental Coding Files
StorePreviousSwitchValues.vi

Click here to access/download
Supplemental Coding Files
TCPRead_Write.vi

Click here to access/download

Supplemental Coding Files

TCPRead_Write_GlobalVariables.vi

Click here to access/download
Supplemental Coding Files
calibrationScript.m

Click here to access/download
Supplemental Coding Files
intensityDetermination.m

Click here to access/download
Supplemental Coding Files
myGUI.m

Click here to access/download
Supplemental Coding Files
plotIntensityCurves.m

[Click here to access/download](#)

Supplemental Coding Files
[regionOfInterestDetermination.m](#)

Click here to access/download
Supplemental Coding Files
selectIntensity.m